LiMETIME:
LINEAR MODEL OF ELECTRIC TRAINS INCLUDING MOTOR EFFICIENCY

A Thesis

by

Burhan Toruk

Submitted to the
Graduate School of Sciences and Engineering
In Partial Fulfillment of the Requirements for
the Degree of

Master of Science

in the
Department of Electrical and Electronics Engineering

Özyeğin University
August 2022

Copyright © 2022 by Burhan Toruk

LiMETIME:
LINEAR MODEL OF ELECTRIC TRAINS INCLUDING MOTOR EFFICIENCY

Approved by:

Prof. H. Fatih Uğurdağ, Advisor
Department of Electrical and Electronics Engineering
Özyeğin University

Prof. Taylan Akdoğan
Department of Electrical and Electronics Engineering
Özyeğin University

Asst. Prof. Onur Demir
Department of Computer Engineering
Yeditepe University

Date Approved: 06 August 2022

To my family, friends and instructors

ABSTRACT

To implement an optimization method that aims to increase energy efficiency, the definition of the vehicle model is crucial to calculate results that can be used in the real-world environment. Component behavior and environmental effects should be included to generate precise output from models. In literature works, authors directly focus on implementing the vehicle model with basic plant models. However, they did not consider the efficiency of the components in the calculation results of optimization methods. In this thesis, an optimization model including energy losses due to the efficiency of the e-machines is implemented to see the effect of component features. The LiMETIME is suitable for different-sized efficiency maps and is implemented using the Mixed Integer Linear Algorithm (MILP) approach. One of the strongest MILP based vehicle model approaches is implemented as the base of the LiMETIME. After that, the efficiency map of the e-machine and inverter is included on top of this. A 5x5 efficiency map is implemented with six different routes to demonstrate the vehicle's behavior. In reality, efficiency values vary between 72-95% for energy-efficient e-machines. Since the efficiency values are set as 100% in literature, the total energy consumption values increased 21% on average in LiMETIME. Execution time is also increased because of the additional constraints and decision variables. The application time obtained in this study is between 8.46 and 90.71 times longer than the literature study.

Keywords: Mixed Integer Linear Programming (MILP), Efficiency, Energy Optimization, Electric Vehicle (EV), Trains

ÖZETÇE

Enerji verimliliğini artırmayı hedefleyen bir optimizasyon yönteminde, gerçek dünya ortamında kullanılabilecek sonuçları elde edebilmek için, araç modeli tanımı oldukça önemlidir. Modellerden kesin çıktılar elde etmek için araç bileşenlerinin davranışları ve çevresel faktörler dahil edilmelidir. Literatürdeki çalışmalarda, yazarlar araç modelini doğrudan temel sistem modelleri ile uygulamaya odaklanmıştır. Ancak bu optimizasyon yöntemlerinin hesaplama sonuçlarında bileşenlerin verimliliğini dikkate almamışlardır. Bu tezde, bileşen özelliklerinin etkisini görmek için elektrik makinelerinin verimliliğinden kaynaklanan enerji kayıplarını da içeren bir optimizasyon modeli uygulanmıştır. LiMETIME, farklı büyüklükteki verimlilik haritaları için uygundur ve Karma Tam Sayılı Doğrusal Algoritma (MILP) yaklaşımını kullanmaktadır. En güçlü MILP tabanlı araç modeli yaklaşımlarından biri LiMETIME'ın temeli olarak uygulanmıştır. Sonrasında bu uygulamanın üzerine elektrik makinesi ve invertörün verimlilik haritası eklenmiştir. Aracın davranışını göstermek için altı farklı rota ile 5x5 boyutlarında bir verimlilik haritası uygulanmıştır. Gerçekte, enerji verimliliği yüksek olan elektrik makineleri için verimlilik değerleri %72-95 arasında değişmektedir. Literatürdeki çalışmada verim değerleri %100 olarak ele alındığından toplam enerji tüketim değerleri LiMETIME için ortalama %21 artmıştır. Ek kısıtlamalar ve karar değişkenleri nedeniyle optimizasyon için geçen süre de artmıştır. Bu çalışmada elde edilen optimizasyon süresi literatür çalışmadan 8,46 ile 90,71 kat arasında daha fazla olarak elde edilmiştir.

Anahtar Kelimeler: Karışık Tamsayılı Doğrusal Programlama (MILP), Verimlilik, Enerji Optimizasyonu, Elektrikli Araç (EV), Trenler

ACKNOWLEDGEMENTS

I would like to sincerely express my thanks to my advisor Prof. H. Fatih Uğurdağ, at Özyeğin University, who helped me a lot before and after I joined his team. The first steps of this work were taken when I was a Teaching Assistant at Özyeğin University. Prof. H. Fatih Uğurdağ helped me to get accepted to Özyeğin University as a teaching assistant with a scholarship. Also, I thank the whole Özyeğin University family for giving me this opportunity.

I am also so grateful to FEV Türkiye and especially M. Ali Gözüküçük. During this work, he was my director and helped me with his automotive and optimization knowledge.

I want to thank my friends for encouraging me during this work. Finally, I would like to thank my family for giving support in every part of my life.

TABLE OF CONTENTS

LIST OF TABLES

LIST OF FIGURES

LIST OF ABBREVIATIONS

EV Electric Vehicle *p.* iv, v, 13

ICE Internal Combustion Engine *p.* 9, 10

MILP Mixed Integer Linear Programming *p.* iv, v, 2, 5, 13–15, 17–20, 27, 28, 31

MLD Mixed Logical Dynamic *p.* 2, 3, 14, 16

PMP Pontryagin Maximum Principle *p.* 2

PWA Piece-wise Approximation *p.* viii, 2, 15, 20–22, 31, 32, 35–37

RPM Rotation per Minute *p.* ix, 10, 11, 13, 19, 20, 22, 23, 25–30, 33, 39–44

CHAPTER I

INTRODUCTION

With the increasing demand for energy and the interest in reducing carbon emissions, it has been a subject that has been studied extensively on reducing energy consumption in transportation systems [7]. It is stated that approximately 28% of the country's energy consumption in the USA is spent on transportation [8, 9]. Similarly, this figure was announced in the UK as about 30% [10]. In the USA, the distribution of transportation energy usage is 58% for cars and light trucks, 5% for medium trucks, 18% for heavy trucks and buses, and 19% for non-highway vehicles [9]. Among the many means of transport, the usage of railways is expected to increase further. Railway vehicles are efficient because the resistance between wheels and rail is meager. Moreover, railways offer comfort, reliability, high transport capacity [11]. 60-70% of the total energy spent on the railway is spent on the movement of the trains [12]. This energy includes the energy needed for traction or braking, motion resistance, environmental conditions, and auxiliary loads like air conditioning and illumination [13]. EU emphasized that increasing the efficiency of railway systems is very important from an environmental and economic point of view. Due to this, they highlighted that any improvement has to be done [14]. This is why reducing the energy consumption of the railway transportation system is essential and can be possible by increasing efficiency.

To date, many studies have been proposed to optimize the speed trajectory to increase the energy efficiency of vehicles. Many different methods have been proposed to achieve this under different situations. Speed trajectory optimization belongs to a basic principle: finding a good speed profile with traction, regenerative braking, coasting, and mechanical braking [15]. Many research papers aim to minimize energy consumption by finding optimal speed trajectory using different methodologies like ant colony algorithm, genetic algorithm, and linear programming in [16–19]. Also, The Pontryagin Maximum Principle (PMP) in the optimization method is applied to optimizing the speed trajectory in [20, 21]. To locate the speed trajectory, the MILP approach has been used in studies previously. However, in [16, 22], the main limitation is that the speed trajectory must be monotonous. In [15], non-linear parameters were added to the model by using piecewise approximation to overcome this issue. This paper's main contribution is overcoming the speed trajectory's monotonicity. So, this methodology can deal with both acceleration and deceleration processes. In the study [6], the aim is to minimize energy consumption by optimizing the speed trajectory. Since non-linear train operation model is converted to mixed logical dynamic (MLD) model by using piece-wise affine (PWA) approximations, this study supports the acceleration and deceleration process of the vehicle. Moreover, this work includes a feature called the passenger comfort parameter. This parameter limits the acceleration and deceleration force for better passenger comfort. The vehicle must complete the journey by a strict deadline, so this method also supports time-constrained routes. However, energy losses due to e-machine and inverter are ignored as other linear vehicle optimization models using MILP in literature. Because of the addition of comfort parameter and time constraint, this work was chosen as the base of LiMETIME, and it is called 'literature work' in this paper.

The proposed method in this paper offers flexibility and robustness. The main contribution of LiMETIME is including e-machine and inverter losses in calculations compared with previous linear vehicle models. Therefore, this model is much closer to realistic situations. By adding an efficiency map, the model can be used to calculate energy consumption on the battery or power supply input of the vehicle.

The structure of this paper can be described as follows. The problem is described in the later part of this chapter, and some background knowledge is mentioned. Chapter II covers the implementation of the mixed logical dynamic model

(MLD). After that, the addition of the efficiency lookup table on the MLD model is introduced. Chapter III demonstrates case studies in six different route profiles. Chapter IV is the conclusion of this work and contains an introduction to future work.

1.1 Problem Description

This study aims to produce a linear vehicle model which includes the energy lost due to electric motor, transmission, and other powertrain components. Also, it aims to minimize energy consumption in a pre-defined route by using this linear model.

Every system in our life can be expressed as a dynamic model, including a vehicle. The dynamic model of a vehicle is described according to the following equations in the literature [6]:

$$m\rho\frac{dv}{dt} = u_{tb}(t) + R_b(v) + R_{line}(s) \qquad \frac{ds}{dt} = v$$

m: Mass (kg)

ρ: Rotating mass factor

v: Vehicle speed (m/s)

s: Position (m)

u_{tb}: is the control variable (traction/braking force)

R_b: Basic resistance contains air drag and rolling resistances

R_{line}: Total line resistance contains track grade, curve, and tunnel resistances

u_{tb} is limited to between the minimum traction force (u_{min}) and maximum traction force (u_{max}).

Due to Strahl formula [23], the basic resistance R_b is defined as follows:

$$R_b(s) = m(a_1 + a_2v^2)$$

a_1 and a_2 are calculated by collecting real-life vehicle data by driving test. These values depend on the materials of the wheel, road, and wind speed. The line resistance $R_{line}(s)$ is due to the slope, curves, and tunnels and can be included in the model. In this study, road profiles were chosen as straight and without a tunnel. That is why the line resistance $R_{line}(s)$ is formulated simpler such that it includes resistance due to slope only:

$$R_{line}(s) = mgsin\alpha(seg)$$

$\alpha(seg)$: Segment slope

g: The gravitational acceleration (m/s^2)

The optimal control problem of vehicle motion can be defined as linear. u_{tb} is defined as a control variable for the traction and braking force of the vehicle. Distance s and speed v are defined as the state values. Generally, the optimization problem is described as solving for 'minimum time' or 'minimum energy in a limited trip time.' In this paper, the optimization problem is defined to solve for minimum energy in a limited trip time (T_{max}). Furthermore, motor efficiency and passenger comfort will be considered [24].

$$J = \int_0^T n(u_{tb}(t)v(t) + \lambda \left|\frac{du_{tb}(t)}{dt}\right|)dt \to min$$

J is the objective function defined by the total amount of energy consumption in a deadline and the sum of riding comfort. By including the riding comfort part, transitions and rate of change are reduced on traction force (u_{tb}). n is the motor and powertrain efficiency coming from the efficiency map.

As Franke et al. [25], the kinetic energy per mass ($E_k = 0.5v^2$) unit is used to decrease the calculation complexity and eliminate model non-linearities due to the terms like v^2.

$$m\rho\frac{dE_k}{dt} = u_{tb}(s) - R_b(\sqrt{2E_k}) - R_{line}(s) \qquad \frac{dt}{ds} = \frac{1}{\sqrt{2E_k}} \tag{1}$$

Optimization problem is specified as follows:

$$J = \int_{s_{start}}^{s_{end}} n(u_{tb}(s) + \lambda. \left|\frac{du_{tb}(s)}{dt}\right|)ds \rightarrow min \tag{2}$$

And boundary conditions can be written as follows:

$$u_{min} \leq u_{tb}(s) \leq u_{max}$$

$$0 \leq E_k(s) \leq E_{max}(s)$$

$$E(s_{start}) = E_{start}, \quad E(s_{end}) = E_{end}, \quad t(s_{start}) = 0, \quad t(s_{end}) = T_{max}$$

$$E_{max}(s) = 0.5V_{max}(s)^2$$

u_{min}: Minimum traction force value that vehicle can achieve

u_{max}: Maximum braking force value that vehicle can achieve

v_{max}: The maximum speed that vehicle can achieve

s_{start}: Starting position

s_{end}: Final position

E_{start}: Starting kinetic energy (J)

E_{end}: Final kinetic energy (J)

In the end, this problem is an optimization problem. Adding powertrain efficiency (n) into this optimization problem is essential.

1.2 Background Knowledge

In this section, there is knowledge about deterministic vehicle models, critical reasons for the electric motor loss and MILP is explained briefly. These pieces of information are handy for understanding further details. For example, the torque calculation in the linear model is directly related to the deterministic vehicle model.

1.2.1 Physical Equations of Vehicle Model

During the travel of a vehicle, many different forces show positive or negative effects on vehicle movement. Also, these forces affect the total energy consumption.

This section will briefly describe the deterministic vehicle energy consumption model and related physical formulas [26]. Also, free-body diagram of a vehicle can be seen in Figure 1 which is showing the the forces that consuming energy. In this section, equations are based on energy but in Figure 1, corresponding forces can be seen.

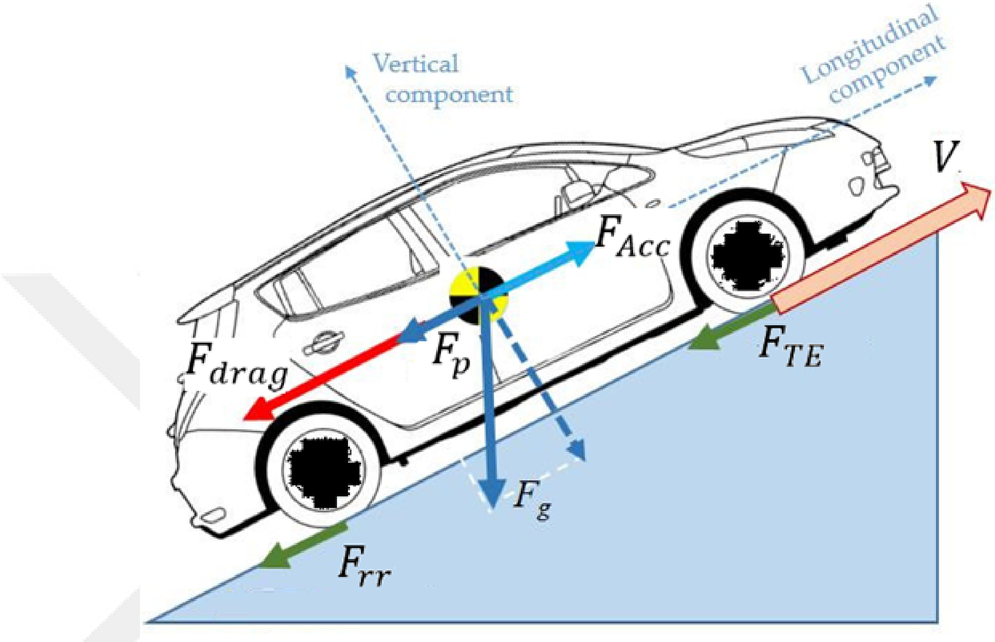

Figure 1: The forces that effecting vehicle movement [1].

- Average Speed (V_{AV}, m/s)

  To calculate the consumed energy in a segment or road part, the average speed of that segment should be calculated.

$$V_{AV} = \frac{V_{in} + V_f}{2}$$

  V_{in}: Segment initial speed (m/s)

  V_f: Segment final speed (m/s)

- Combined Drag Coefficient (C_{comb})

  Combined Drag Coefficient is a quantity that depends on three constants. It should be calculated to get the energy loss due to the air resistance.

$$C_{comb} = \frac{1}{2}\rho C_D A$$

ρ: Air Density (kg/m^3)

C_D: Drag Coefficient

A: Vehicle Frontal Area (m^2)

Then E_{drag} can be calculated. It represents the amount of energy investigation due to the vehicle's aerodynamic structure and is related to the work against air resistance.

$$E_{drag} = C_{comb} V_{AV}^2$$

E_{drag} : Drag (Air Resistance) Energy Loss (J)

- Acceleration Energy (Kinetic Energy) Loss/Gain (E_{Acc}, J)

  This formula calculates the difference between initial and final kinetic energies. The result of this formula can be positive or negative. This negativity means that there is an energy gain called regeneration.

$$E_{Acc} = \frac{m}{2}(V_f^2 - V_{in}^2)$$

m: Vehicle mass (kg)

- Potential Energy (Ascent) Loss/Gain (E_p, J)

  This formula calculates the potential energy difference between the initial and final points of the segment. Also, the result of this formula can be positive or negative.

$$E_p = mgsin(arctan(slope))V_{AV}$$

g: Acceleration of gravity (m/s^2)

$slope$: The slope between start and end point

- Rolling Resistance Energy Loss (E_{RR}, J)

  Rolling resistance is another force that opposes the motion. It always resists body rolling and depends on parameters such as tire resistance and camber angles.

$$E_{RR} = mgC_{RR}V_{AV}$$

  C_{RR}: Vehicle rolling resistance coefficient

- Tire Rotational Inertia Energy Loss (E_{TE}, J)

  Angular velocity (ω) calculation is needed to calculate the energy loss due to the tire rotational inertia.

$$\omega = \frac{V}{r}$$

  ω: Angular velocity (s^{-1})

  V: Vehicle speed (m/s)

  r: Wheel radius (m)

  The movement of the tire generates a force against the rotation direction. The amount of energy consumed due to this force can be calculated using the following formula.

$$E_{TE} = \frac{1}{2} In_{wheel}(\omega_f^2 - \omega_{in}^2)n$$

  In_{wheel}: Wheel inertia of one wheel (kgm^2)

  ω_{in}: Initial angular velocity (s^{-1})

  ω_f: Final angular velocity (s^{-1})

  n: Number of wheels

- Total Consumed/Gained Energy at the Wheel (E_{wheel}, J)

  Total consumed or gained energy can be calculated by the following formula.

$$E_{wheel} = E_{drag} + E_{Acc} + E_p + E_{RR} + E_{TE}$$

- Efficiency

  Cumulative efficiency (n) can be calculated by multiplying motor and transmission efficiency. While transmission efficiency is a constant manufacturer value, motor efficiency is gathered from a map.

$$n = n_{tr} n_m$$

  n_{tr}: Vehicle transmission/powertrain efficiency

  n_m: Motor Efficiency (from efficiency map)

- Total Consumed/Gained Energy at the Battery (E_{batt}, J)

  To calculate the energy on the battery side, efficiency should find a place in the calculation. Two equations should define this because efficiency (n) should be used in different places. While gained energy at the battery is less than gained energy at the wheel, it is the opposite for consumed energy.

$$E_{batt-out} = \frac{E_{wheel}}{n}$$

$$E_{batt-in} = nE_{wheel}$$

  $E_{batt-out}$: Consumed energy from battery (J)

  $E_{batt-in}$: Gained energy from battery (J)

1.2.2 Efficiency of Electric Motor vs Internal Combustion Engine

An electric motor is much more efficient than an internal combustion engine (ICE). To date, the most efficient ICE for a vehicle is from Mercedes-AMG's Formula 1 team, which has 50% thermal efficiency. Nevertheless, it is known that this engine is not road legal. Mercedes and Mazda are working on more efficient road legal ICE's with an efficiency of 41% and 56% respectively [27]. When these values are compared with the massive 90% thermal efficiency of vehicle electric motors, the result of this comparison becomes clear [28]. This is why, this thesis focuses on electric vehicles.

1.2.3 Losses in Electric Motor

This section defines the reason for energy loss in electric motors and why there is an efficiency map to cover this part. Electric motor losses can be divided into mechanical or electrical.

- Mechanical Losses

  Mechanical losses can be caused by bearing friction and wind resistance (windage) due to the spinning rotor. Bearings of rotating parts are covered with grease oil. Therefore, the frictional loss is like a cubic function of rotor speed (RPM). If there were only air instead of oil, the frictional loss would be linear to RPM. Variation of frictional power loss against speed can be seen in Figure 2.

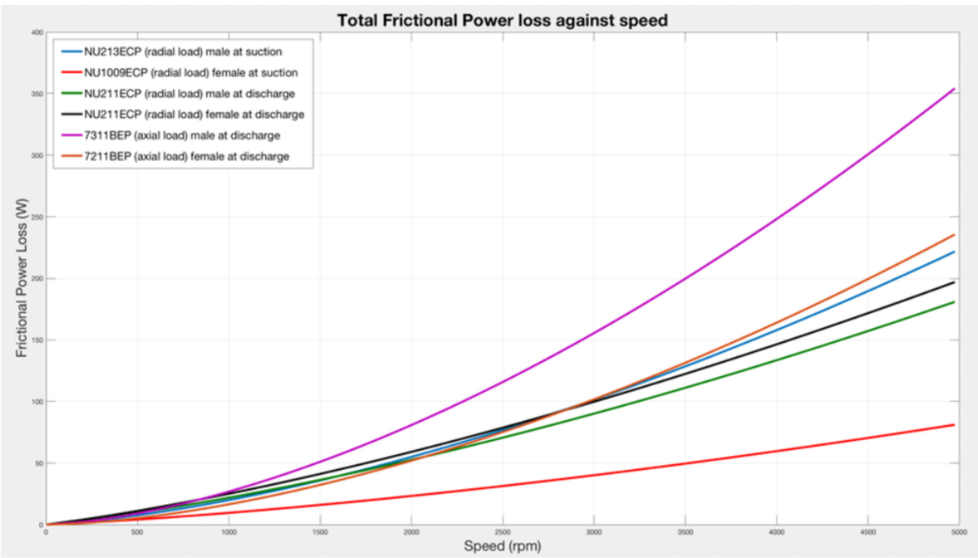

Figure 2: Bearing friction loss for six different bearing [2].

Bearing friction can be defined as follows, moment M gets supplied from four sources [29]:

$$M = M_{rr} + M_{sl} + M_{seal} + M_{drag}$$

where M_{rr} is the rolling frictional moment (Nmm), M_{sl} is the sliding frictional moment (Nmm), M_{seal} is the frictional moment from integral seals (Nmm), M_{drag} is the frictional moment from drag losses (Nmm).

Windage is caused by air displacement around rotating parts of an electric motor. It is one of the most energy consumers and is also not linear to RPM. This loss increases dramatically when RPM increases. Windage loss agains speed can be seen in Figure 3.

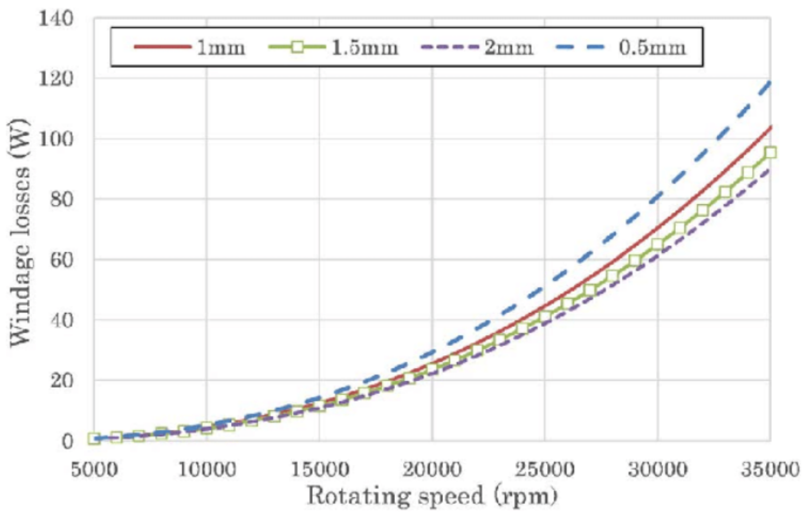

Figure 3: Windage loss for different air gaps [3].

- Electrical Losses

  Electrical losses can be divided into three major categories: core losses, stator resistance (I^2R) losses, rotor resistance (I^2R) losses, and stray load losses. Core materials have resistance against changing magnetic fields. Also, it creates eddy currents. Some amount of energy is getting consumed to overcome these oppositions. This loss is called core loss.

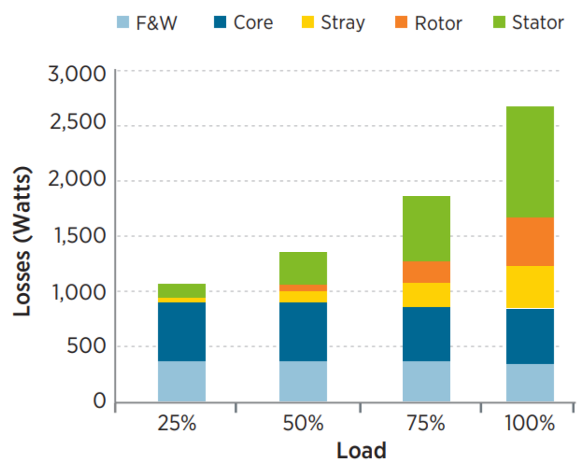

Figure 4: Losses compered with motor load for a standard motor [4].

Stator and rotor losses are produced when there is current flow through them. This flow creates heat, and it means that there is an energy loss. Stray load losses are getting generated by leakage fluxes.

I^2R losses and stray losses are proportional to motor load. I^2R losses can drop motor efficiency to around 0% when the vehicle barely moves [28, 30]. The distribution of electrical losses for different loads can be checked in Figure 4.

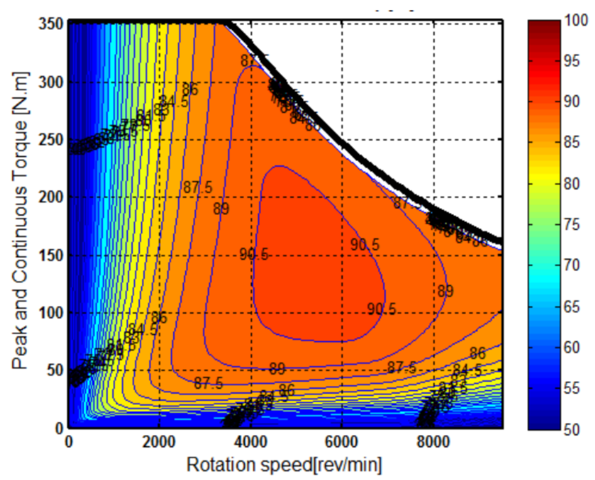

Figure 5: Efficiency map example [5].

- Efficiency Map

  In previous sections, it mentioned five main energy loss factors. These effects depend on the speed and load/torque of the electric motor. That is why the efficiency of an electric machine is represented as a map. The axis of this 2D map is torque and RPM. For example, the efficiency map of an EV's electric motor can be seen in Figure 5.

1.2.4 Mixed Integer Linear Programming

An integer linear programming problem is a mathematical optimization and feasibility check problem in which some or all of the decision variables are forced to be integers. In this programming methodology, the objective function and constraints must be linear.

If only some of the decision variables are not an integer, the problem is called the MILP problem, which also includes some continuous decision variables [31].

The standard form of integer linear programming is shown as follows:

$$\begin{aligned} c^T x \rightarrow \text{maximize/minimize} \quad & \text{(Objective Function)} \\ A \cdot x \leq b, \quad & \text{(Bound Constraints)} \\ Aeq \cdot x = beq, \quad & \text{(Linear Constraints)} \\ lbound \leq x \leq ubound, \quad & \text{(Bound Constraints)} \\ x \in \mathbb{Z}^n, \quad & \text{(Integrity Constraints)} \end{aligned}$$

In linear programming problems, the aim is to find optimal decision variables that make the objective function value the highest or lowest possible. This possibility is called feasibility. The Branch-and-Bound algorithm is used for optimization, but in the past, this algorithm improved by proposing new methods called Presolve, Cutting Planes, Heuristics, and Parallelism [32].

CHAPTER II

IMPLEMENTATION OF LiMETIME

In this chapter, the implementation of LiMETIME is described. In section 2.1, it will be discussed the conversion of the non-linear vehicle model to Mixed Logical Dynamic (MLD) model. This conversion part is taken from literature work [6]. After that, the addition of the efficiency lookup table (map) is explained in section 2.2.

2.1 The Mixed Logical Dynamic Model

In this section, it is described that how a vehicle control problem can be converted to Mixed Logical Dynamic (MLD) model. By doing this conversion, the model can be solved with (MILP). This approach is suggested by Wang et al. [6]. Dividing the whole route into segments (seg) is used in many studies to get a discrete model like Franke et al. [25].

The line resistance $R_{line}(seg)$, which includes segment slope only, can be calculated before the optimization. It is a fixed value for each segment because the route is pre-defined. The segment number i can take values between one and the total number of segments (N_r).

$$R_{line}(seg) = R_{line,i} \quad \text{for} \quad seg \in [seg_i, seg_{i+1}]$$

In previous chapters, it has been mentioned that using kinetic energy instead of speed is an excellent way to linearize the problem. The motion equation 1 should be revised by using kinetic energy (E_k):

$$\frac{dE_k}{dseg} = \frac{1}{m\rho} u_{tb}(i) - \frac{a_2}{\rho} E_k(seg) - \frac{1}{\rho}(a_1 + R_{line,i})$$

Putting simple coefficients is possible because there are constant for each interval. This operation makes this differential function much simpler as well:

$$\frac{dE_k}{dseg} = \zeta u_{tb}(i) + \eta E_k(seg) + \gamma_i$$
$$\zeta = \frac{1}{m\rho}, \quad \eta = -\frac{a_2}{\rho}, \quad \gamma_i = -\frac{1}{\rho}(a_1 + R_{line,i})$$

The next segment's kinetic energy value $E_k(i+1)$ can be found by solving this differential equation. It possible to put the linear relationship between the current and next segment's kinetic energy values into the model by doing this. Instead of $E_k(seg_i)$, $E_k(i)$ was written for simplicity:

$$E_k(i+1) = \epsilon^{\eta\Delta seg_i} E_k(i) + (\epsilon^{\eta\Delta seg_i} - 1)\frac{\zeta}{\eta} u_{tb}(i) + (\epsilon^{\eta\Delta seg_i} - 1)\frac{\gamma_i}{\eta}$$

The optimization problem is time limited. So, the vehicle should finish the route efficiently in a certain amount of time. Due to this, segment time and route time calculations become mandatory. The time is gathered from kinetic energy by calculating the differential equations and trapezoidal integration rule [33]. However, there is a time limit (T_{max}), and this rule should be implemented into the model by two constraints. The time equation and these constraints can be shown as follows:

$$t(i+1) = t(i) + \frac{1}{2}\left(\frac{1}{\sqrt{2E_k(i)}} + \frac{1}{\sqrt{2E_k(i+1)}}\right)\Delta seg_i \tag{3}$$

$$t(1) = 0, \quad t(seg_{end}) = T_{max}$$

It is known that all operations have to be linear for MILP approach. However, there are square-root operations in the time equation 3 which are not linear. In this case, using piece-wise approximation (PWA) is a good option, as Azuma et al. [34] suggested. In this work, this non-linear part is defined with three linear functions, and their coefficients are calculated by using least-squares optimization [6]. The PWA approximation on non-linear time function can be checked in Figure 6. Function $f_{PWA}(E_k) = \frac{1}{2\sqrt{2E_k}}$ can be defined as follows:

$$f_{PWA}(E_k) = \begin{cases} \alpha_1 E_k(i) + \beta_1 & \text{for} \quad E_{min} \leq E_k(i) \leq E_{k1} \\ \alpha_2 E_k(i) + \beta_2 & \text{for} \quad E_{k1} \leq E_k(i) \leq E_{k2} \\ \alpha_3 E_k(i) + \beta_3 & \text{for} \quad E_{k2} \leq E_k(i) \leq E_{max} \end{cases}$$

The effect of approximation error can be reduced by adding more linear functions. However, this addition will increase the execution time of optimization. The non-linear time dynamics equation (3) can be rewritten as follows:

$$t(i+1) = t(i) + (\alpha_l E_k(i) + \beta_l + \alpha_m E_k(i+1) + \beta_m)\Delta seg_i$$

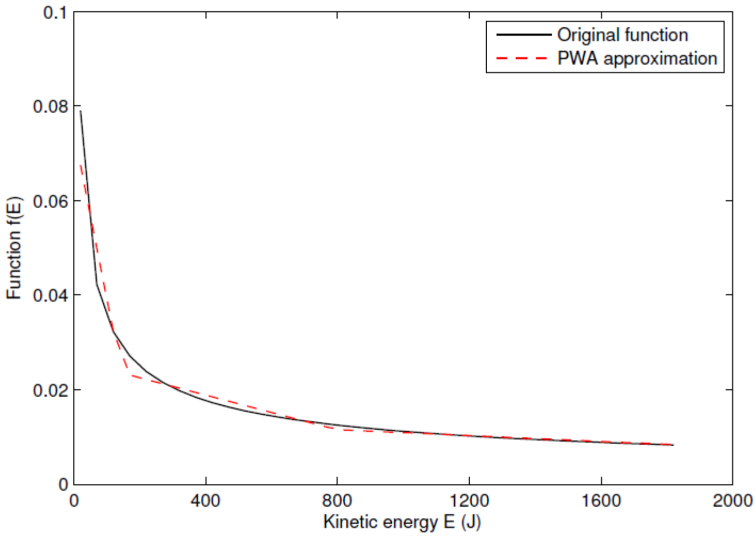

Figure 6: PWA approximation of $f_{PWA}(E_k) = \frac{1}{2\sqrt{2E_k}}$ [6].

There are three regions and two borders between them. Three binary variables should be presented to convert this approximation equation to MLD model. These variables detect E_k's placement in the three regions. These variables ($\delta_1(i)$ and $\delta_2(i)$) can be shown as follows [35]:

$$[E_k(i) < E_{k1}] \Leftrightarrow [\delta_1(i) = 1]$$

$$[E_k(i) < E_{k2}] \Leftrightarrow [\delta_2(i) = 1]$$

$E_k(i)$ can not be less than E_{min} and more than E_{max}. To detect which region that $E_k(i)$ belongs, following constraints should be added into the model [35]:

$$
\begin{aligned}
(E_{max} - E_{k1})\delta_1(i) &\leq E_{max} - E_k(i) \\
(E_{min} - E_{k1})\delta_1(i) &\leq E_k(i) - E_{k1} \\
(E_{max} - E_{k2})\delta_2(i) &\leq E_{max} - E_k(i) \\
(E_{min} - E_{k2})\delta_2(i) &\leq E_k(i) - E_{k2}
\end{aligned}
\tag{4}
$$

It is possible to cover two regions with previous non-linearities 4. But there is another region between E_{min} and E_{k1}. So, $E_k(i)$ can be smaller than both E_{k1} and E_{k2}. That is why a third binary variable $\delta_3(i)$ is needed. This new binary variable is equal to product of $\delta_1(i)$ and $\delta_2(i)$. It's not possible to define $\delta_3(i) = \delta_1(i)\delta_2(i)$ operation as it is, because this is not linear. It can be performed by following inequalities [35]:

$$
\begin{aligned}
-\delta_1(i) + \delta_3(i) &\leq 0 \\
-\delta_2(i) + \delta_3(i) &\leq 0 \\
\delta_1(i) + \delta_2(i) - \delta_3(i) &\leq 1
\end{aligned}
\tag{5}
$$

Also, $\delta(i)E_k(i)$ product is needed for this optimization problem. This operation can not be implemented directly with MILP. Three new continuous variables is proposed as $z_1(i) = \delta_1(i)E_k(i)$, $z_2(i) = \delta_2(i)E_k(i)$ and $z_3(i) = \delta_3(i)E_k(i)$. These operations can be done by implementing these constraints [35]:

$$
\begin{aligned}
z_j(i) &\leq E_{max}\delta_j(i) \\
z_j(i) &\geq E_{min}\delta_j(i) \\
z_j(i) &\leq E_k(i) - E_{min}(1 - \delta_j(i)) \\
z_j(i) &\geq E_k(i) - E_{max}(1 - \delta_j(i))
\end{aligned}
\tag{6}
$$

After all of these definitions and constraints, $\alpha_j E_k(i) + \beta_j$ can be defined as follows for $j = \{1, 2, 3\}$:

$$\alpha_j(i)E_k(i) + \beta_j = [-\alpha_3 \;\; \alpha_2 - \alpha_3 \;\; \alpha_1 - \alpha_2 + \alpha_3]\, z(i)$$
$$+ [-\beta_3 \;\; \beta_2 - \beta_3 \;\; \beta_1 - \beta_2 + \beta_3]\, \delta(i)$$
$$+\alpha_3 E_k(i) + \beta_3$$

$$z(k) = [z_1(k) \;\; z_2(k) \;\; z_3(k)]^T$$
$$\delta(k) = [\delta_1(k) \;\; \delta_2(k) \;\; \delta_3(k)]^T$$

By using the sum of products, the objective function (2) is redefined as follows:

$$J = n(\sum_{i=1}^{N_r} u_{tb}(i)\Delta seg_i + \sum_{i=1}^{N_r-1} \lambda \left|\Delta u_{tb}(i)\right|) \tag{7}$$

Absolute value operation breaks linearity for negative numbers. That is why it is not an option to put directly into the MILP model. That's why, there should be another variable $Y = |\Delta u_{tb}(i)|$. By using this variable, this operation can be implemented. Following inequalities should be added:

$$Y(i) \geq u_{tb}(i+1) - u_{tb}(i)$$
$$Y(i) \geq u_{tb}(i) - u_{tb}(i+1)$$

After this objective function (7) can be rewritten as:

$$J = n(\sum_{i=1}^{N_r} u_{tb}(i)\Delta seg_i + \sum_{i=1}^{N_r-1} \lambda Y)$$

After these operations, the dynamic model turned into a linear model. Because of objective function and all constraints are linear, this problem can be solved with MILP. There are continuous variables like u_{tb}, Y, z as well as binary variables like δ. This is where the 'mixed' term comes from. In a route, there can be different speed limits and different slopes in some parts. That is why the route should be separated into segments. Because, in this methodology, there can not be different slopes or speed limits in a single segment. If it is taken as there is N_r segments, the segment identification number should take values as $i = \{1, 2, 3, \cdots, N_r\}$. To work with many segments, all binary and continuous variables should be identified as vectors as follows:

$$\hat{u_{tb}} = \begin{bmatrix} u_{tb}(1) \\ u_{tb}(2) \\ \vdots \\ u_{tb}(N_r) \end{bmatrix}, \quad \hat{\delta_j} = \begin{bmatrix} \delta_j(1) \\ \delta_j(2) \\ \vdots \\ \delta_j(N_r+1) \end{bmatrix}, \quad \hat{Y} = \begin{bmatrix} Y(1) \\ Y(2) \\ \vdots \\ Y(N_r-1) \end{bmatrix}, \quad \hat{z_j} = \begin{bmatrix} z_j(1) \\ z_j(2) \\ \vdots \\ z_j(N_r+1) \end{bmatrix}$$

In this section, the implementation of a dynamic model of a vehicle is described. The model is not dealing with powertrain efficiency yet. The efficiency map implementation part will be described in the next chapter. These applications can be developed and executed by using solvers like CPLEX, Xpress, and MATLAB Optimization Toolbox.

2.2 Addition of Efficiency Lookup Table

In this section, the addition of an efficiency map is described with all needed constraints and equations. In this study, a 5x5 lookup table is used, but the size can be increased by extending the equations. This chapter consists of two sections. Torque and RPM calculation will be described in the first section, then getting the actual efficiency from the map will be explained.

2.2.1 Calculation of Torque and RPM

The axes of an efficiency map are divided based on torque and RPM. In this case, torque and RPM calculation can be done in the linear model. To do this dynamic calculation, two new continuous variables are proposed, which are TRQ and RPM. Torque calculation is straightforward, and its equation is already suitable for MILP approach:

$$TRQ = u_{tb}(\frac{r_{tyre}}{Ri_f})$$

r_{tyre}: Tyre radius (m)

Ri_f: Final drive ratio

This equation can be converted to linear inequalities as follows:

$$TRQ \leq u_{tb}(\frac{r_{tyre}}{Ri_f})$$
$$TRQ \geq u_{tb}(\frac{r_{tyre}}{Ri_f})$$

Tire radius and final drive ratio values are vehicle specific. Exact values should be taken from manufacturers. Dynamic motor rotation per minute (RPM) calculation in a linear model is much more complicated than torque calculation. RPM equation can be shown as follows:

$$RPM = \frac{60 \cdot Ri_f \cdot v}{2 \cdot \pi \cdot r_{tyre}} \tag{8}$$

In equation 8, all variables are constant except vehicle speed (v). As it has been known from previous chapters, in this study, kinetic energy (E_k) is used instead of vehicle speed to protect linearity. There is no linear equation to directly get vehicle speed from kinetic energy or relocation. Time is a continuous decision variable, and it is calculated dynamically in this linear model. It means it is impossible to do something like relocation over time. This operation can not be executed with the MILP approach. In this situation, piece-wise approximation (PWA) comes handy again. By doing this, the MILP approach can calculate vehicle speed from kinetic energy. PWA function of vehicle speed $g_{PWA}(v) = \sqrt{2E_k}$ can be defined as follows:

$$g_{PWA}(v) = \begin{cases} \alpha_{v1}E_k(i) + \beta_{v1} & \text{for} \quad E_{min} \leq E_k(i) \leq E_{kv1} \\ \alpha_{v2}E_k(i) + \beta_{v2} & \text{for} \quad E_{kv1} \leq E_k(i) \leq E_{kv2} \\ \alpha_{v3}E_k(i) + \beta_{v3} & \text{for} \quad E_{kv2} \leq E_k(i) \leq E_{max} \end{cases}$$

$$E_{min} < E_{kv1} < E_{kv2} < E_{max}$$

Also, this PWA approach consists of three regions. That's why, three new binary decision variables ($\delta_4(i)$, $\delta_5(i)$ and $\delta_6(i)$) should be defined. After that, the same operations done for the first PWA approximation should be performed respectively. These equations are not written here again for simplicity, but they can be seen by checking equations 4, 5, 6.

For this second PWA approach, using the same kinetic energy borders can decrease complexity and would improve execution time at the same time. If this way is chosen, there is no need to define new binary variables. Same $\delta_1(i)$, $\delta_2(i)$ and $\delta_3(i)$ can be used here also. Only coefficients of PWA functions should be calculated again, because there is a different function at all. The PWA approximation on non-linear speed function can be seen in Figure 7. To use same kinetic energy borders, the following conditions should be satisfied:

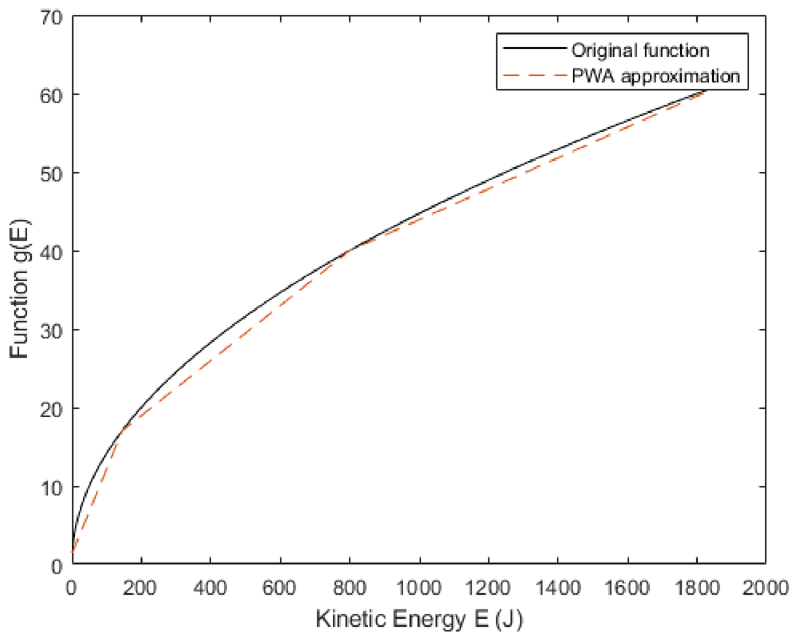

Figure 7: PWA approximation of $g_{PWA}(E_k) = \sqrt{2E_k}$.

$$E_{k1} = E_{kv1}$$

$$E_{k2} = E_{kv2}$$

After this PWA approximation, speed values can be calculated without non-linear operations. When these speed values are named as v_{PWA}, RPM formula can be written as follows:

$$RPM = \frac{60 \cdot Ri_f \cdot v_{PWA}}{2 \cdot \pi \cdot r_{tyre}}$$

After the PWA approximation operation, the accuracy of speed calculation for a dummy road can be seen in Table 1.

Table 1: Accuracy of PWA approximation of speed.

# of Occurrence	Exact Speed (m/s)	PWA Speed (m/s)	Difference (%)
2	0	1.31	100
1	9.93	6.65	49.28
1	11.75	8.79	33.70
1	13.98	11.89	17.51
1	16.70	16.42	1.69
15	17.03	17.02	0.032
Average			5.40

The average difference value in Table 1 is calculated concerning the number of occurrences in the dummy route. Also, the places where the vehicle speed is zero are taken as an outlier.

2.2.2 Efficiency Calculation

After torque and RPM calculation, the ‘true’ efficiency values can be obtained from the efficiency map. This section mentions the calculation of efficiency values for an efficiency map with five rows and five columns. The dummy efficiency map can be seen in Table 2.

Table 2: Dummy efficiency map.

		RPM				
		$< rpm1$	$< rpm2$	$< rpm3$	$< rpm4$	$< rpm5$
TORQUE	$< trq1$	90.11	90.12	90.13	90.14	90.15
	$< trq2$	90.21	90.22	90.23	90.24	90.25
	$< trq3$	90.31	90.32	90.33	90.34	90.35
	$< trq4$	90.41	90.42	90.43	90.44	90.45
	$< trq5$	90.51	90.52	90.53	90.54	90.55

The efficiency values were selected specially to check the truth of the methodology. Using these kinds of organized values makes it much easier to check which efficiency values were chosen from which part of the efficiency map.

The axis of the map is torque and RPM. These values are constants and can be presented as $\{rpm1, rpm2, rpm3, rpm4, rpm5\}$ for RPM axis, $\{trq1, trq2, trq3, trq4, trq5\}$ for the torque axis.

Notation of this table can be explained as follows:

$$trq1 < TRQ < trq2 \ \ \& \ \ rpm2 < RPM < rpm3 \Rightarrow n = 90.23$$

$$trq3 < TRQ < trq4 \ \ \& \ \ rpm1 < RPM < rpm2 \Rightarrow n = 90.42$$

TRQ: Calculated torque (Nm)

RPM: Calculated RPM

n: Efficiency

In linear programming, using conditions such as the 'IF' operation is impossible. That is why a similar approach from the previous chapter should be applied to locate calculated torque and RPM on the map. 10 new binary decision variables should be defined as $\{d_{rpm}1, d_{rpm}2, d_{rpm}3, d_{rpm}4, d_{rpm}5\}$ for RPM, $\{d_{trq}1, d_{trq}2, d_{trq}3, d_{trq}4, d_{trq}5\}$ for torque:

$TRQ < trq1 \Rightarrow d_{trq}1 \ \& \ d_{trq}2 \ \& \ d_{trq}3 \ \& \ d_{trq}4 \ \& \ d_{trq}5 = 1$

$TRQ < trq2 \Rightarrow d_{trq}2 \ \& \ d_{trq}3 \ \& \ d_{trq}4 \ \& \ d_{trq}5 = 1$

$TRQ < trq3 \Rightarrow d_{trq}3 \ \& \ d_{trq}4 \ \& \ d_{trq}5 = 1$

$TRQ < trq4 \Rightarrow d_{trq}4 \ \& \ d_{trq}5 = 1$

$TRQ < trq5 \Rightarrow d_{trq}5 = 1$

These equations can be converted to linear inequalities. trq_{max} is the maximum torque, and trq_{min} is the minimum torque value that the vehicle is capable of. These values should be obtained from the data sheet of the vehicle provided by the manufacturer. Following constraints should be added to the model:

$$
\begin{aligned}
(trq_{max} - trq1) \cdot d_{trq}1(i) &\leq trq_{max} - TRQ(i) \\
(trq_{min} - trq1) \cdot d_{trq}1(i) &\leq TRQ(i) - trq1 \\
(trq_{max} - trq2) \cdot d_{trq}2(i) &\leq trq_{max} - TRQ(i) \\
(trq_{min} - trq2) \cdot d_{trq}2(i) &\leq TRQ(i) - trq2 \\
(trq_{max} - trq3) \cdot d_{trq}3(i) &\leq trq_{max} - TRQ(i) \\
(trq_{min} - trq3) \cdot d_{trq}3(i) &\leq TRQ(i) - trq3 \\
(trq_{max} - trq4) \cdot d_{trq}4(i) &\leq trq_{max} - TRQ(i) \\
(trq_{min} - trq4) \cdot d_{trq}4(i) &\leq TRQ(i) - trq4 \\
(trq_{max} - trq5) \cdot d_{trq}5(i) &\leq trq_{max} - TRQ(i) \\
(trq_{min} - trq5) \cdot d_{trq}5(i) &\leq TRQ(i) - trq5
\end{aligned}
\tag{9}
$$

Binary decision variables of RPM can be expressed as follows:

$$RPM < rpm1 \Rightarrow d_{rpm}1 \ \ \& \ \ d_{rpm}2 \ \ \& \ \ d_{rpm}3 \ \ \& \ \ d_{rpm}4 \ \ \& \ \ d_{rpm}5 = 1$$
$$RPM < rpm2 \Rightarrow d_{rpm}2 \ \ \& \ \ d_{rpm}3 \ \ \& \ \ d_{rpm}4 \ \ \& \ \ d_{rpm}5 = 1$$
$$RPM < rpm3 \Rightarrow d_{rpm}3 \ \ \& \ \ d_{rpm}4 \ \ \& \ \ d_{rpm}5 = 1$$
$$RPM < rpm4 \Rightarrow d_{rpm}4 \ \ \& \ \ d_{rpm}5 = 1$$
$$RPM < rpm5 \Rightarrow d_{rpm}5 = 1$$

Similar to the torque, linear inequalities of binary RPM decision variables can be shown as follows. rpm_{max} is the maximum RPM, and rpm_{min} is the minimum RPM value. While rpm_{max} can be calculated from maximum vehicle speed, rpm_{min} should be taken as zero:

$$\begin{gathered}
(rpm_{max} - rpm1) \cdot d_{rpm}1(i) \leq rpm_{max} - RPM(i) \\
(-rpm1) \cdot d_{rpm}1(i) \leq RPM(i) - rpm1 \\
(rpm_{max} - rpm2) \cdot d_{rpm}2(i) \leq rpm_{max} - RPM(i) \\
(-rpm2) \cdot d_{rpm}2(i) \leq RPM(i) - rpm2 \\
(rpm_{max} - rpm3) \cdot d_{rpm}3(i) \leq rpm_{max} - RPM(i) \\
(-rpm3) \cdot d_{rpm}3(i) \leq RPM(i) - rpm3 \\
(rpm_{max} - rpm4) \cdot d_{rpm}4(i) \leq rpm_{max} - RPM(i) \\
(-rpm4) \cdot d_{rpm}4(i) \leq RPM(i) - rpm4 \\
(rpm_{max} - rpm5) \cdot d_{rpm}5(i) \leq rpm_{max} - RPM(i) \\
(-rpm5) \cdot d_{rpm}5(i) \leq RPM(i) - rpm5
\end{gathered} \tag{10}$$

After the operations 9 and 10, the binary decision values can be found as example in Table 3. Due to the design of the operation, it is seen that the binary values are becoming true more than once for the same route segment. Because, if any RPM value is lower than $rpm3$, it's also lower than $rpm4$ and $rpm5$.

While finding the corresponding efficiency value from the map with respect to the torque and RPM, these binary decision variables are becoming essential. By checking these values, the algorithm will be able to check which part of the efficiency map should be brought. Nevertheless, these binary values are confusing. They should be getting into a form that only the border is true. For example, if RPM value is lower than $rpm3$, only $d_{rpm}3$ value should be true, and all other decision binary variables should be false.

A simple extraction operation can do this operation. It is not breaking the linearity as well. To do this, ten new binary decision variables should be proposed as $\{dr_{rpm}1, dr_{rpm}2, dr_{rpm}3, dr_{rpm}4, dr_{rpm}5\}$ for RPM and similarly, $\{dr_{trq}1, dr_{trq}2, dr_{trq}3, dr_{trq}4, dr_{trq}5\}$ for torque.

Table 3: Example of torque binary decision variables.

Example	$d_{trq}1$	$d_{trq}2$	$d_{trq}3$	$d_{trq}4$	$d_{trq}5$
$TRQ < trq1$	1	1	1	1	1
$TRQ < trq2$	0	1	1	1	1
$TRQ < trq3$	0	0	1	1	1
$TRQ < trq4$	0	0	0	1	1
$TRQ < trq5$	0	0	0	0	1

When Table 3 and Table 4 are compared, the operation is looking like finding diagonal of matrix. This function ($diag$) is available in MATLAB, but the linear programming approach does not accept it. That is why the following constraints should be used to revise binary decision values:

$$dr_{trq}1 \leq d_{trq}1 \qquad dr_{rpm}1 \leq d_{rpm}1$$

$$dr_{trq}1 \geq d_{trq}1 \qquad dr_{rpm}1 \geq d_{rpm}1$$

$$dr_{trq}2 \leq d_{trq}2 - d_{trq}1 \qquad dr_{rpm}2 \leq d_{rpm}2 - d_{rpm}1$$

$$dr_{trq}2 \geq d_{trq}2 - d_{trq}1 \qquad dr_{rpm}2 \geq d_{rpm}2 - d_{rpm}1$$

$$dr_{trq}3 \leq d_{trq}3 - d_{trq}2 \qquad dr_{rpm}3 \leq d_{rpm}3 - d_{rpm}2$$

$$dr_{trq}3 \geq d_{trq}3 - d_{trq}2 \qquad dr_{rpm}3 \geq d_{rpm}3 - d_{rpm}2$$

$$dr_{trq}4 \leq d_{trq}4 - d_{trq}3 \qquad dr_{rpm}4 \leq d_{rpm}4 - d_{rpm}3$$

$$dr_{trq}4 \geq d_{trq}4 - d_{trq}3 \qquad dr_{rpm}4 \geq d_{rpm}4 - d_{rpm}3$$

$$dr_{trq}5 \leq d_{trq}5 - d_{trq}4 \qquad dr_{rpm}5 \leq d_{rpm}5 - d_{rpm}4$$

$$dr_{trq}5 \geq d_{trq}5 - d_{trq}4 \qquad dr_{rpm}5 \geq d_{rpm}5 - d_{rpm}4$$

The tables are similar for RPM. Due to this, the tables about RPM decision variables were not placed here.

Table 4: Example of revised torque binary decision variables.

Example	$dr_{trq}1$	$dr_{trq}2$	$dr_{trq}3$	$dr_{trq}4$	$dr_{trq}5$
$TRQ < trq1$	1	0	0	0	0
$TRQ < trq2$	0	1	0	0	0
$TRQ < trq3$	0	0	1	0	0
$TRQ < trq4$	0	0	0	1	0
$TRQ < trq5$	0	0	0	0	1

MILP is an optimization algorithm, and it converges to optimum values step by step. Nevertheless, converging exactly to an integer value is difficult, especially for complex problems. During optimization, the difference between optimized value and integer value decreases. Some tolerances are added to make a solution in a shorter time or be able to find a solution. One of which is named integer tolerance. By adding this, the MILP algorithm can stop when the difference between the optimized value and nearest integer is lower than the tolerance.

These tolerances can cause some problems as well. For example, after execution, binary values can get real values around 0 and 1. A round operation can be needed to deal with these non-binary issues. Rounding can be done simply by using *round* function in MATLAB. However, this is not suitable for MILP. The same result can be obtained by implementing the followings:

$$\begin{aligned} (0.5) \cdot dr_{round} &\leq 1 - dr \\ (-0.6) \cdot dr_{round} &\leq dr - 0.5 \end{aligned} \tag{11}$$

In equation 11, dr_{round} is rounded binary decision variable, dr is binary decision variable before rounding. These constraints can be applied to both the torque and RPM side.

After rounding the binary decision variables, the efficiency value can be found by checking the places where both torque and RPM binary decision values are true. As it has known that the 'IF' function is not available in linear programming, two-dimensional matrix multiplication and multiplication of two decision variables are not possible. That is why a unique form is needed here. All binary decision variables should be collected in a vector form. Furthermore, the efficiency map should be reshaped for this unique form. This form can be seen for a 5x5 efficiency map and a route with 20 segments in Table 5.

Table 5: The unique form for a route with $N_r = 20$ segments.

$\vec{dt}_{trq}$	$\vec{dt}_{rpm}$	Efficiency Vector
$\vec{dr}_{trq}1$	$\vec{dr}_{rpm}1$	$[90.11, 90.11, \cdots, 90.11]_{N_r \times 1}$
$\vec{dr}_{trq}1$	$\vec{dr}_{rpm}2$	$[90.12, 90.12, \cdots, 90.12]_{N_r \times 1}$
$\vec{dr}_{trq}1$	$\vec{dr}_{rpm}3$	$[90.13, 90.13, \cdots, 90.13]_{N_r \times 1}$
$\vec{dr}_{trq}1$	$\vec{dr}_{rpm}4$	$[90.14, 90.14, \cdots, 90.14]_{N_r \times 1}$
$\vec{dr}_{trq}1$	$\vec{dr}_{rpm}5$	$[90.15, 90.15, \cdots, 90.15]_{N_r \times 1}$
$\vec{dr}_{trq}2$	$\vec{dr}_{rpm}1$	$[90.21, 90.21, \cdots, 90.21]_{N_r \times 1}$
$\vec{dr}_{trq}2$	$\vec{dr}_{rpm}2$	$[90.22, 90.22, \cdots, 90.22]_{N_r \times 1}$
$\vec{dr}_{trq}2$	$\vec{dr}_{rpm}3$	$[90.23, 90.23, \cdots, 90.23]_{N_r \times 1}$
$\vec{dr}_{trq}2$	$\vec{dr}_{rpm}4$	$[90.24, 90.24, \cdots, 90.24]_{N_r \times 1}$
$\vec{dr}_{trq}2$	$\vec{dr}_{rpm}5$	$[90.25, 90.25, \cdots, 90.25]_{N_r \times 1}$
$\vec{dr}_{trq}3$	$\vec{dr}_{rpm}1$	$[90.31, 90.31, \cdots, 90.31]_{N_r \times 1}$
$\vec{dr}_{trq}3$	$\vec{dr}_{rpm}2$	$[90.32, 90.32, \cdots, 90.32]_{N_r \times 1}$
$\vec{dr}_{trq}3$	$\vec{dr}_{rpm}3$	$[90.33, 90.33, \cdots, 90.33]_{N_r \times 1}$
$\vec{dr}_{trq}3$	$\vec{dr}_{rpm}4$	$[90.34, 90.34, \cdots, 90.34]_{N_r \times 1}$
$\vec{dr}_{trq}3$	$\vec{dr}_{rpm}5$	$[90.35, 90.35, \cdots, 90.35]_{N_r \times 1}$
$\vec{dr}_{trq}4$	$\vec{dr}_{rpm}1$	$[90.41, 90.41, \cdots, 90.41]_{N_r \times 1}$
$\vec{dr}_{trq}4$	$\vec{dr}_{rpm}2$	$[90.42, 90.42, \cdots, 90.42]_{N_r \times 1}$
$\vec{dr}_{trq}4$	$\vec{dr}_{rpm}3$	$[90.43, 90.43, \cdots, 90.43]_{N_r \times 1}$
$\vec{dr}_{trq}4$	$\vec{dr}_{rpm}4$	$[90.44, 90.44, \cdots, 90.44]_{N_r \times 1}$
$\vec{dr}_{trq}4$	$\vec{dr}_{rpm}5$	$[90.45, 90.45, \cdots, 90.45]_{N_r \times 1}$
$\vec{dr}_{trq}5$	$\vec{dr}_{rpm}1$	$[90.51, 90.51, \cdots, 90.51]_{N_r \times 1}$
$\vec{dr}_{trq}5$	$\vec{dr}_{rpm}2$	$[90.52, 90.52, \cdots, 90.52]_{N_r \times 1}$
$\vec{dr}_{trq}5$	$\vec{dr}_{rpm}3$	$[90.53, 90.53, \cdots, 90.53]_{N_r \times 1}$
$\vec{dr}_{trq}5$	$\vec{dr}_{rpm}4$	$[90.54, 90.54, \cdots, 90.54]_{N_r \times 1}$
$\vec{dr}_{trq}5$	$\vec{dr}_{rpm}5$	$[90.55, 90.55, \cdots, 90.55]_{N_r \times 1}$

Two new binary decision values should be defined to be able to produce this special form. These values are $\vec{dt}_{trq}$ for torque and $\vec{dt}_{rpm}$ for RPM. These two variables keep all binary decision forms as shown in Table 5. The number of route segments is defined as N_r and the dimensions of the efficiency map is $q \times w$. With these, dimensions of these variables can be imagined as follows:

$$\vec{dr_{trq}1} = \begin{bmatrix} dr_{trq}1(1) \\ dr_{trq}1(2) \\ \vdots \\ dr_{trq}1(N_r) \end{bmatrix}, \quad \vec{dr_{rpm}1} = \begin{bmatrix} dr_{rpm}1(1) \\ dr_{rpm}1(2) \\ \vdots \\ dr_{rpm}1(N_r) \end{bmatrix}, \quad \vec{dt_{trq}} = \begin{bmatrix} dt_{trq}(1) \\ dt_{trq}(2) \\ \vdots \\ dt_{trq}(N_r \cdot q \cdot w) \end{bmatrix}$$

$$\vec{dt_{rpm}} = \begin{bmatrix} dt_{rpm}(1) \\ dt_{rpm}(2) \\ \vdots \\ dt_{rpm}(N_r \cdot q \cdot w) \end{bmatrix}, \quad \vec{d_{chosen}} = \begin{bmatrix} dt_{trq}(1) \cdot dt_{rpm}(1) \\ dt_{trq}(2) \cdot dt_{rpm}(2) \\ \vdots \\ dt_{trq}(N_r \cdot q \cdot w) \cdot dt_{rpm}(N_r \cdot q \cdot w) \end{bmatrix}$$

A multiplication operation should be performed to find where both torque and RPM decision variable is true. Another decision value is created and named d_{chosen}. Thanks to this, only the mentioned parts became true. But, due to the multiplication of two decision variables is not applicable, the following non-linearities should be implemented instead of multiplication:

$$\begin{aligned} -dt_{trq}(i) + d_{chosen}(i) &\leq 0 \\ -dt_{rpm}(i) + d_{chosen}(i) &\leq 0 \\ dt_{trq}(i) + dt_{rpm}(i) - d_{chosen}(i) &\leq 1 \end{aligned}$$

Element-wise multiplication of reshaped efficiency values and d_{chosen} gives another vector that every $q \cdot w$ element is for a segment, respectively. For example, if there is a 5x5 efficiency map, every group consists of 25 elements. There is only one value that is different from zero in this element group, which is the efficiency value for the respective segment. Result of the addition of $q \cdot w$ elements respectively, a vector that includes the efficiency values for each segment can be found.

CHAPTER III

CASE STUDY

In this chapter, the lookup table implemented MILP model is applied to different routes with different segment lengths, numbers, and grades. The energy consumption results and execution time are compared as well. It should be clarified that the implementation is done using Optimization Toolbox, MATLAB R2020b, and a computer with a 3.6 GHz 6 core CPU and 16 GB DRAM.

Parameters of the vehicle are chosen concerning the parameters in literature work [6]. These parameters are shown in Table 6.

Table 6: Vehicle parameters.

Parameter	Symbol	Unit	Value
Mass	m	kg	7.10^5
Basic Resistance	R_b	N/kg	$0.02 + 4.417 \cdot 10^{-5}$
Mass factor	ρ	-	1.06
Maximum speed	V_{max}	m/s	50
Maximum Traction Force	u_{max}	N	$4 \cdot 10^5$
Minimum Traction Force	u_{min}	N	$-3 \cdot 10^5$

In this work, there are two PWA approximations. The coefficients of these approximations are given in Table 7 for time and Table 8 for speed calculation. In both, their non-linear graphs are divided into three regions. These values are used to perform studies. The kinetic energy (E) intervals are chosen as the same to reduce complexity.

The comfort parameter λ is 500. This value is the same as literature work [6].

Table 7: PWA coefficients for time calculation.

Region m	a_m	b_m	E_m
1	$-0.3525 \cdot 10^{-3}$	0.0746	$0-145$
2	$-0.0184 \cdot 10^{-3}$	0.0262	$145-800$
3	$-0.0031 \cdot 10^{-3}$	0.0140	$800-1250$

Table 8: PWA coefficients for speed calculation.

Region vm	a_{vm}	b_{vm}	E_{vm}
1	0.1084	1.306	$0-145$
2	0.0351	11.944	$145-800$
3	0.0197	24.259	$800-1250$

All routes are divided into segments into these case studies to achieve a discrete model. Conditions like road grade, air flow rate, traction and braking force, and train parameters are assumed to be as same within a segment. Route length, the time limit (T_{max}), and grade are differentiated between routes.

Table 9: Efficiency map (%).

		RPM				
		< 600	< 1200	< 1800	< 2400	< 3000
TORQUE	< 0	117.6 (85)	117.6 (85)	117.6 (85)	117.6 (85)	117.6 (85)
	< 15000	85	90	92	92	92
	< 30000	82	89	90	93	93
	< 45000	78	88	88	92	93
	< 60000	74	85	85	90	90

The efficiency values are given in Table 9. If there is energy gain which is named regeneration during travel, vehicle torque becomes negative. The table includes a negative torque part to cover this. In this part, efficiency is taken as constant and more than 100%. Because the raw energy values get divided by efficiency, efficiency should have a negative effect in all cases. 1 over 85 equals around 117.6.

While the RPM goes up to 3000, this limit is 60000 for torque. These values can be taken from technical specs and should be the maximum values that a vehicle can achieve. In this case study, six different route profiles were used. While the first route was straight, others had different grade profiles. Furthermore, the route lengths and route time limits were chosen differently. All routes have 20 segments with different segment lengths as well. The comfort value which limits the traction force was chosen as 500 for all cases. The grade profiles, route time limit (seconds), route lengths, and segment lengths (meters) are given in Table 10.

Table 10: Grade profiles and details of the routes.

Route	Length	Seg. Length	Time Limit	Grade Profile
1	10000	500	600	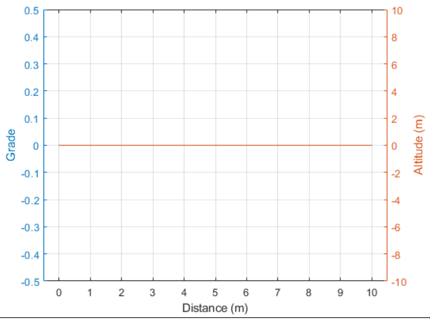
2	10000	500	600	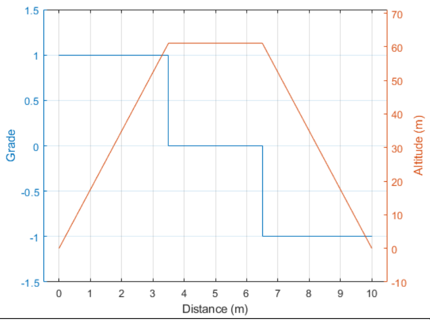
3	10000	500	500	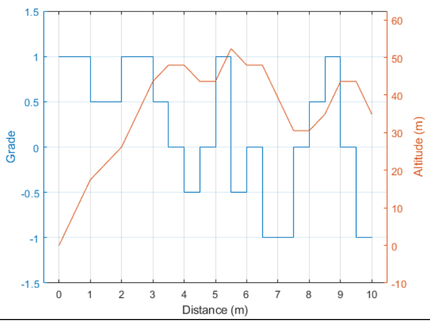

Route	Length	Seg. Length	Time Limit	Grade Profile
4	15000	750	490	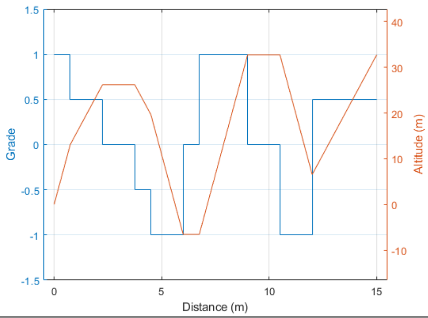
5	8000	400	300	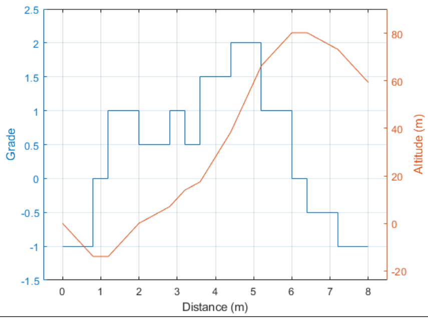
6	12000	600	480	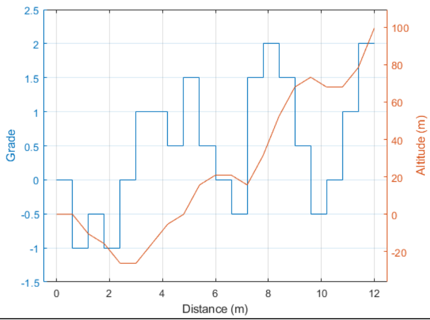

When the final energy consumption of the two approaches is compared, it can be seen that energy consumption is getting increased by adding efficiency values as expected because efficiency can not be 100% due to the losses of converting electric energy to motion. Normalized efficiency values in Table 11 show that the margin is between 1.18 and 1.33. So, adding efficiency increased the energy result by 21% on average. Average efficiency values are calculated from segment's efficiency values by simply finding their mean. These average efficiencies can not prove the normalized energy values because energy consumption is different between segments. However, this can be said that there is a non-linear correlation between these two values.

Table 11: Energy and efficiency comparison between the routes.

	Final Energy (MJ)		Normd. Final Energy		Avg. Eff. (%)
Route	No Eff.	With Eff.	No Eff.	With Eff.	
1	266.79	324.96	1	1.18	89.00
2	386.59	580.13	1	1.33	86.75
3	690.10	929.56	1	1.26	87.70
4	1011.71	1252.95	1	1.19	88.80
5	950.48	1177.38	1	1.19	89.20
6	1100.00	1208.20	1	1.09	91.45
Average			1	1.21	88.82

The comparison between exact speed, which is calculated from kinetic energy (E_k) and speed from PWA approximation in Table 12. As mentioned in the previous chapter, calculating speed from kinetic energy is not a linear operation, which is why PWA approximation was used instead of it. The non-linear function is divided into three regions, but the results are not that bad. The difference between average speed values starts from 1.47% and goes up to 6.48%. However, this should be clarified that an increase in region number decreases the difference.

Table 12: Comparison of exact speed and PWA speed.

Route	Avg. Exact Speed (m/s)	Avg. PWA Speed (m/s)	Difference (%)
1	14.66	14.37	1.97
2	14.66	14.37	1.97
3	24.03	22.47	6.48
4	34.78	34.27	1.47
5	30.93	30.17	2.47
6	28.14	27.27	3.09

The execution time (run-time) results can be checked in Table 13. The increase in the number of constraints is increased the system load dramatically. There is no correlation or linearity between time values. They are specific to the problem itself. Also, it depends on the computer specifications. In this case, the execution time values were multiplied between 8.46 and 90.71 after adding a 5x5 efficiency map.

Table 13: Comparison of execution time.

Route	No Eff. Exec. Time (s)	With Eff. Exec. Time (s)	Normd. Time
1	32.66	375.6	11.50
2	33.61	758.67	22.57
3	10.70	90.48	8.46
4	32.47	246.45	7.59
5	2.5	72.44	28.98
6	3.25	294.82	90.71

The graphical results are placed in Appendix A. There are six graphs for each route. These graphs can be explained as follows:

(a) Speed/Distance Graph: Exact speed and PWA approximated speed can be compared for same route and same methodology.

(b) Route Time/Distance Graph: Increase in route time and its limitation can be seen.

(c) RPM/Distance Graph: Motor rotation speed during travel can be checked.

(d) Torque/Segment Graph: Torque values of each segment can be seen.

(e) Energy/Distance Graph: Increase or decrease in energy values during travel can be checked. Also, this graph can be used to see the difference between no efficiency and energy results that includes efficiency.

(f) Efficiency/Segment Graph: The efficiency value of each segment is shown in this graph.

CHAPTER IV

CONCLUSION

LiMETIME (a linear vehicle model including an efficiency map) is introduced in this thesis. This methodology demonstrates how to implement a non-linear efficiency map to a linear vehicle model. Compared with the literature work [6], total energy consumption values increased 21% on average because of adding powertrain losses to the model. Moreover, LiMETIME is more complex than literature work. The number of constraints and decision variables of the linear model increased dramatically. To be exact, literature work was implemented by using 35 constraints. This number is 76 constraints for LiMETIME. Due to this complex addition to the linear vehicle model, the execution time is also longer, and it is more than the literature, between 8.46 and 90.71 times. On the other hand, the addition of powertrain losses did not affect the speed profiles due to the time constraint of the routes. All essential decision variables, including comparison of exact and PWA approximated speed profiles, are placed in Appendix as graphs, and it is possible to check the correctness of efficiency values by using them.

When the results are examined in this way, it can be thought that LiMETIME is worse than the literature studies both in terms of processing load and in reducing energy consumption, which is its main task. However, it would not be correct to directly compare LiMETIME in this way. Because only LiMETIME has not ignored the motor and inverter efficiency, which is never really 100%. The complexity brought by this account has increased the processing load as expected. Likewise, it is quite normal for studies in the literature that ignore efficiency values to calculate lower energy consumption values.

In this study, the addition of the efficiency map did not affect the speed profile.

The reason for this seems to be that a certain time has been given for the completion of the route. Because when the result graphs are examined, it is observed that the speed profile draws an arc in all case studies. However, investigations will continue to find the root cause.

Future improvements on LiMETIME would be lowering the execution time by optimizing the number of constraints and decision variables. Our proposed model can be compared with other train optimization models using different approaches like dynamic programming, genetic algorithm, ant colony algorithm, etc. LiMETIME can be carried to the cloud as back-end code, and an online optimizer can be developed with a user interface. Nevertheless, although some parts require improvement, LiMETIME contributes to linear train vehicle models and provides a robust calculation to improve the energy efficiency of railway systems.

APPENDIX

CASE STUDIES GRAPHIC RESULTS

These graphs can be checked to compare the validity of case study results.

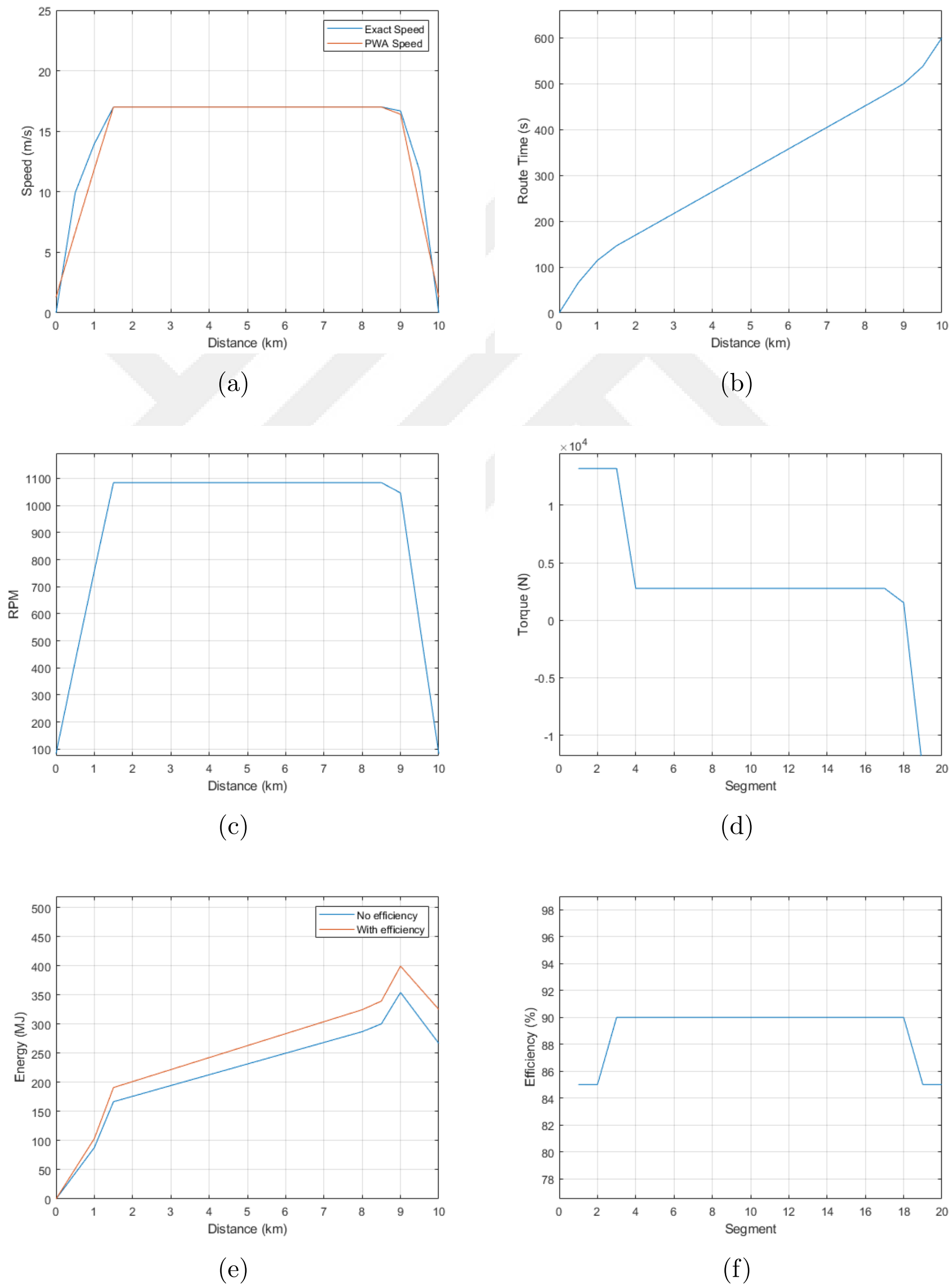

Figure 8: Graphical results of Route 1. (a): Speed. (b): Time. (c): RPM. (d): Torque. (e): Energy. (f): Efficiency.

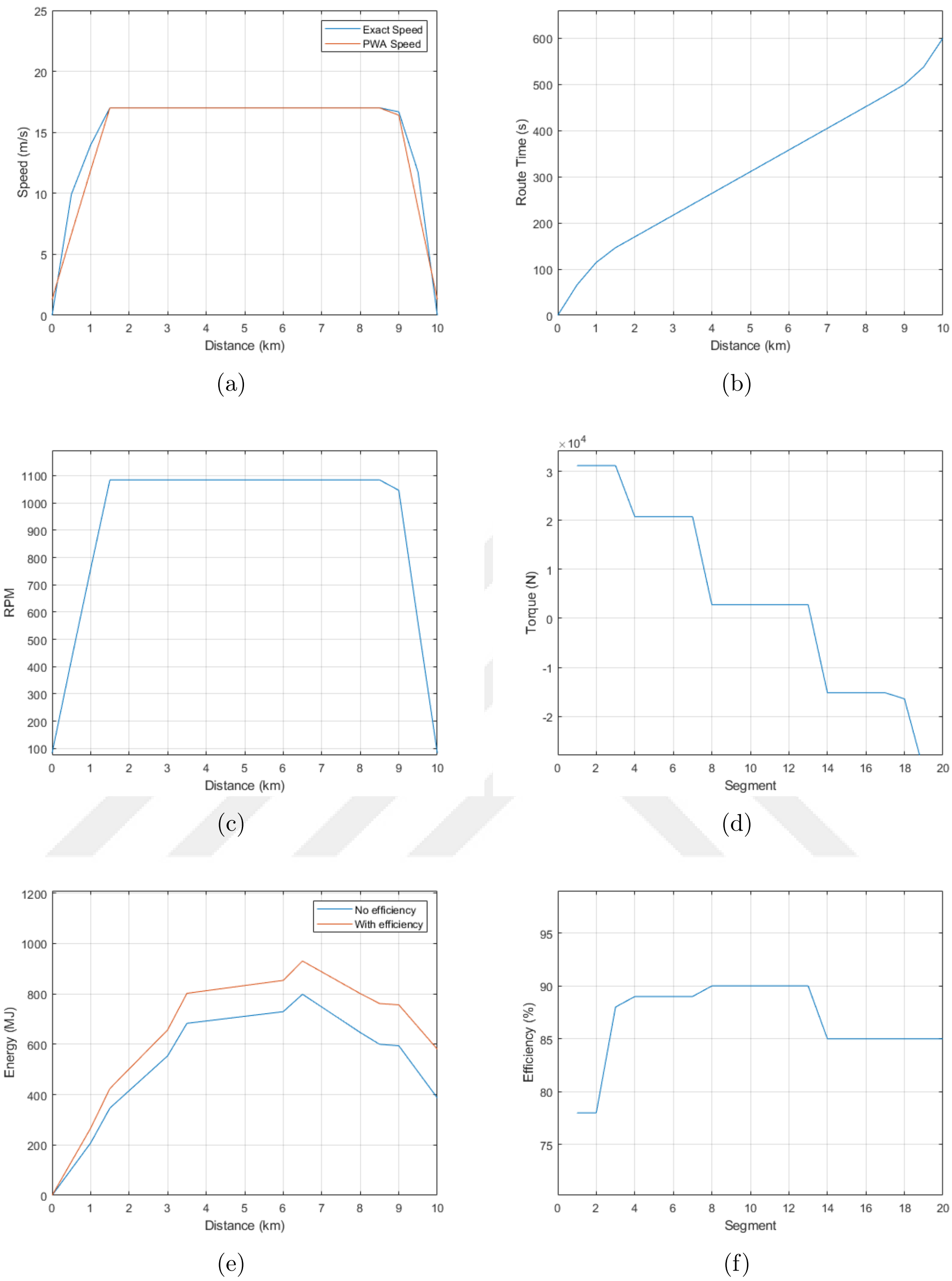

Figure 9: Graphical results of Route 2. (a): Speed. (b): Time. (c): RPM. (d): Torque. (e): Energy. (f): Efficiency.

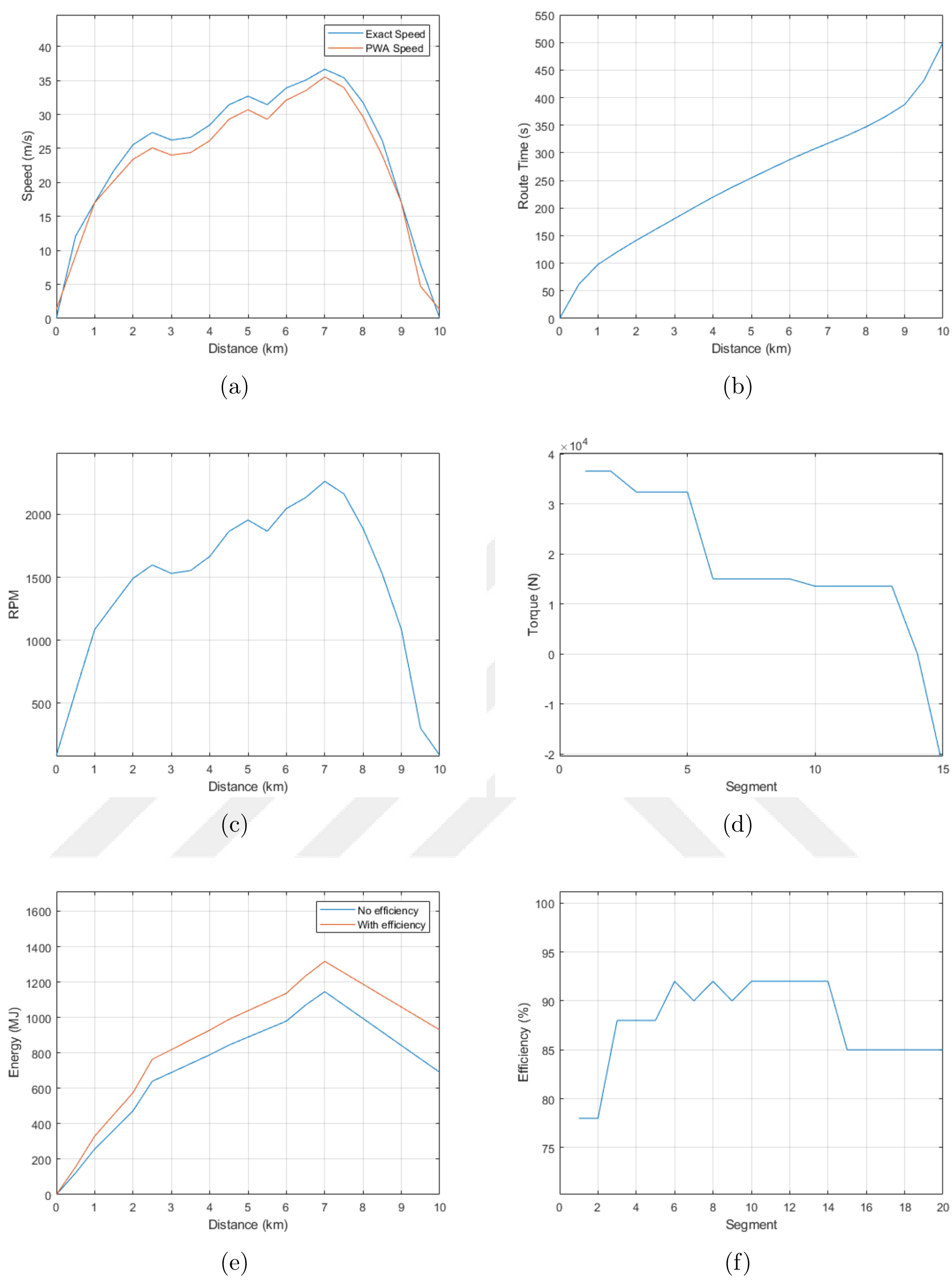

Figure 10: Graphical results of Route 3. (a): Speed. (b): Time. (c): RPM. (d): Torque. (e): Energy. (f): Efficiency.

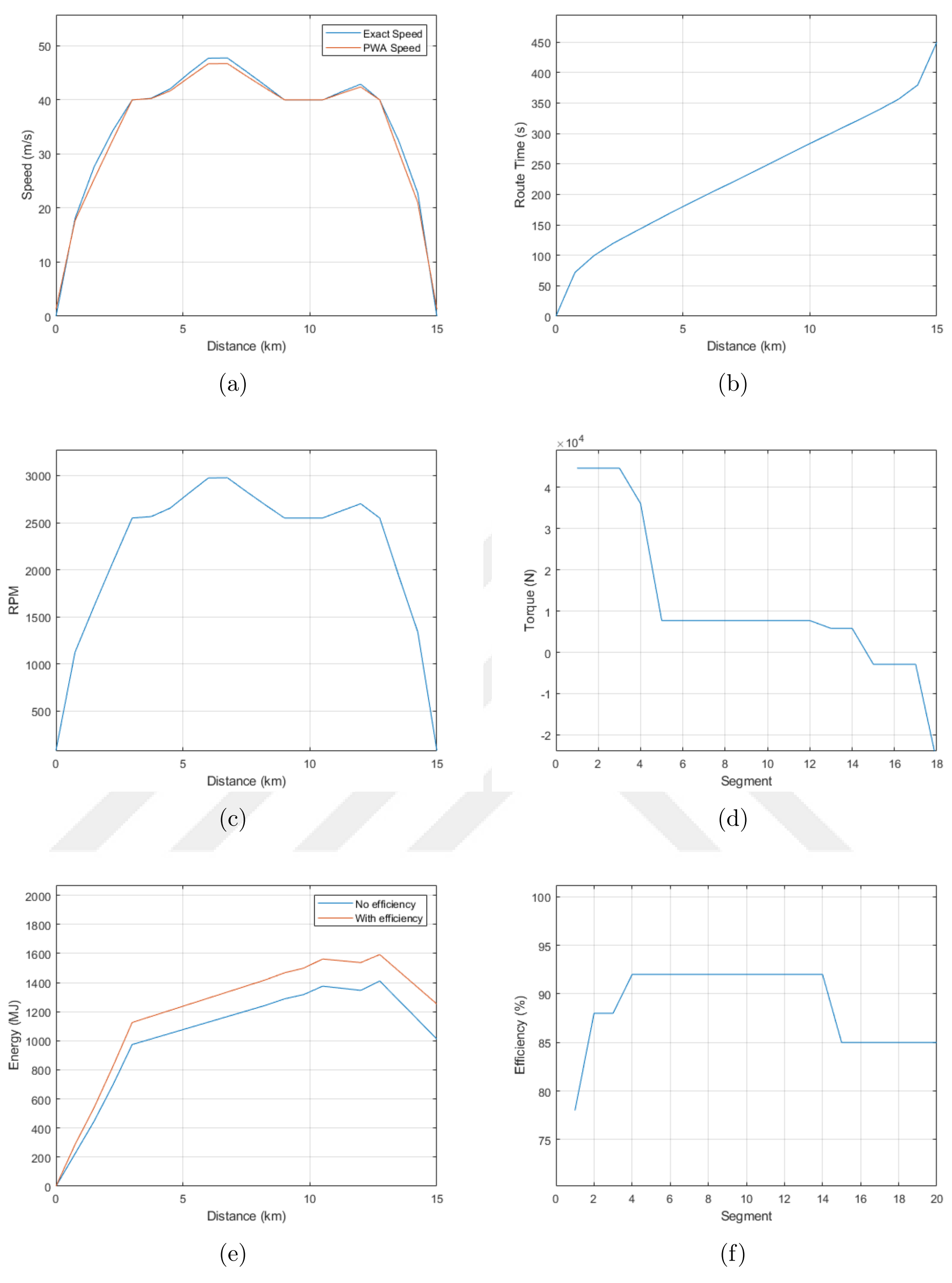

Figure 11: Graphical results of Route 4. (a): Speed. (b): Time. (c): RPM. (d): Torque. (e): Energy. (f): Efficiency.

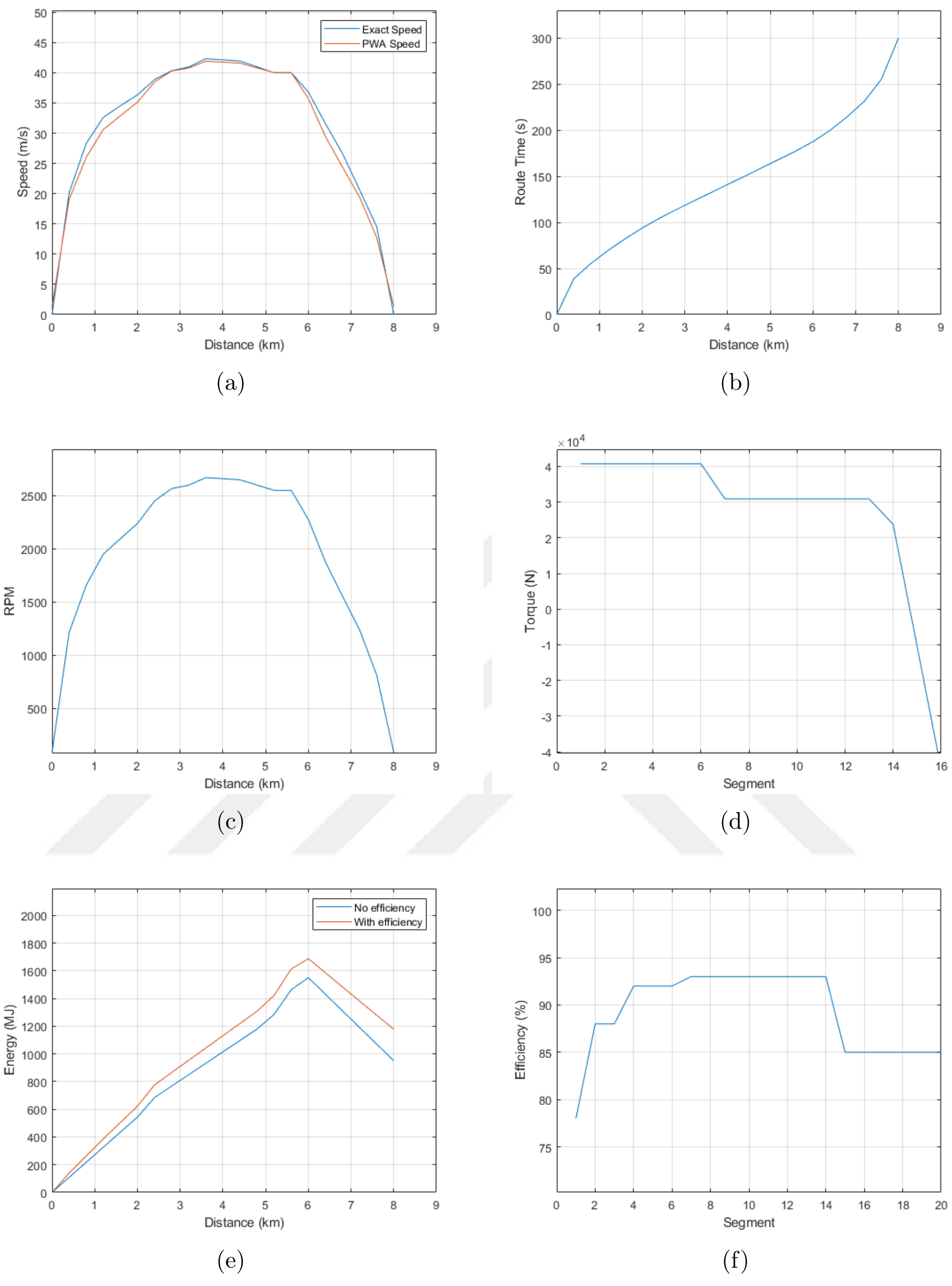

Figure 12: Graphical results of Route 5. (a): Speed. (b): Time. (c): RPM. (d): Torque. (e): Energy. (f): Efficiency.

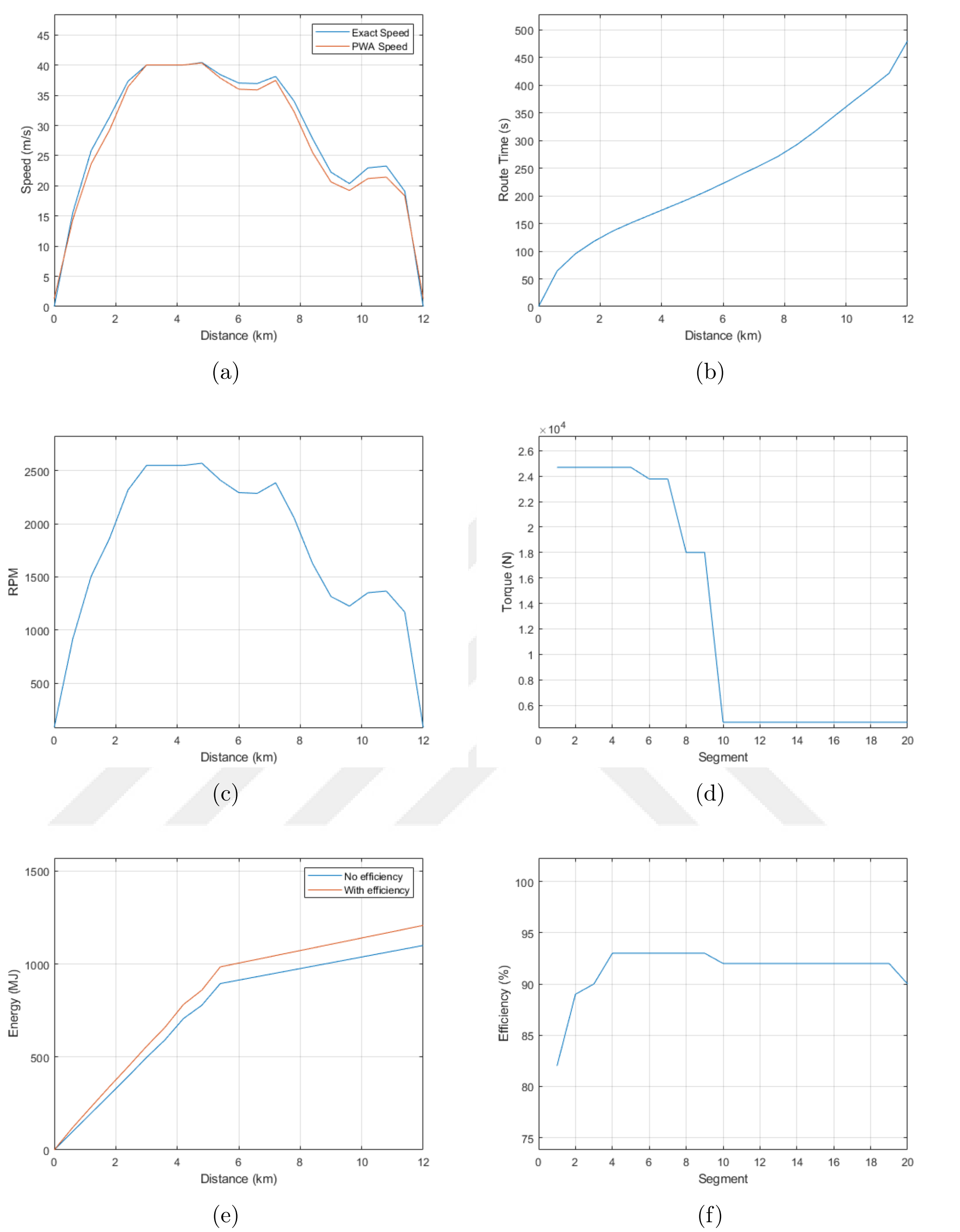

Figure 13: Graphical results of Route 6. (a): Speed. (b): Time. (c): RPM. (d): Torque. (e): Energy. (f): Efficiency.

BIBLIOGRAPHY

[1] D. Jimenez Bermejo, S. Hernandez, J. Fraile-Ardanuy, J. Serrano Romero, R. Pozo, and F. Alvarez, "Modelling the effect of driving events on electrical vehicle energy consumption using inertial sensors in smartphones," *Energies*, vol. 11, p. 412, Feb. 2018.

[2] S. Mukhoryamova, "Analysis and processing of mechanical losses in screw compressors," June 2019.

[3] Z. Xu, A. La Rocca, P. Arumugam, S. Pickering, C. Gerada, S. Bozhko, D. Gerada, and H. Zhang, "A semi-flooded cooling for a high speed machine: Concept, design and practice of an oil sleeve," *43rd Annual Conference of the IEEE Industrial Electronics Society (IECON)*, pp. 8557–8562, Oct. 2017.

[4] G. A. McCoy and J. G. Douglass, "Energy-efficient motor performance and price," in *Energy Efficient Electric Motor Selection Handbook*, Prepared for the U.S. Department of Energy Motor Challenge Program, 1996.

[5] F. Badin, F. Berr, G. Castel, J.-C. Dabadie, H. Briki, P. Dégeilh, and M. Pasquier, "Energy efficiency evaluation of a plug-in hybrid vehicle under european procedure, worldwide harmonized procedure and actual use," *World Electric Vehicle Journal*, vol. 7, pp. 475–488, Sept. 2015.

[6] Y. Wang, B. Ning, T. van den Boom, and B. De Schutter, "Optimal trajectory planning for a single train," *Optimal Trajectory Planning and Train Scheduling for Urban Rail Transit Systems*, pp. 23–51, Sept. 2016.

[7] "UIC and IEA railway handbook 2014-energy consumption and co2 emissions," *Int. Union Railways (IUR)*, 2014. Paris, France.

[8] R. R. Liu and I. M. Golovitcher, "Energy-efficient operation of rail vehicles," *Transportation Research Part A: Policy and Practice*, vol. 37, no. 10, pp. 917–932, 2003.

[9] S. C. Davis and R. G. Boundy, "Transportation energy data book: Edition 40," Feb. 2022.

[10] S. Lechelle and Z. Mouneimne, "Optidrive: A practical approach for the calculation of energy-optimised operating speed profiles," in *IET Conference on Railway Traction Systems (RTS)*, pp. 1–8, 2010.

[11] Y. Wang, B. Ning, F. Cao, B. De Schutter, and T. J. van den Boom, "A survey on optimal trajectory planning for train operations," in *Proceedings of IEEE International Conference on Service Operations, Logistics and Informatics*, pp. 589–594, 2011.

[12] P. Zhou and H. Xu, "Train coordinated optimization operation with regenerative braking," *Journal of Computers*, vol. 7, Apr. 2012.

[13] A. González-Gil, R. Palacin, P. Batty, and J. Powell, "A systems approach to reduce urban rail energy consumption," *Energy Conversion and Management*, vol. 80, pp. 509–524, 2014.

[14] R. Barrero, J. V. Mierlo, and X. Tackoen, "Energy savings in public transport," *IEEE Vehicular Technology Magazine*, vol. 3, no. 3, pp. 26–36, 2008.

[15] Z. Tan, S. Lu, F. Xue, and K. Bao, "A speed trajectory optimization model for rail vehicles using mixed integer linear programming," in *IEEE 20th International Conference on Intelligent Transportation Systems (ITSC)*, pp. 1–6, 2017.

[16] S. Lu, P. Weston, and N. Zhao, "Maximise the regenerative braking energy using linear programming," in *17th International IEEE Conference on Intelligent Transportation Systems (ITSC)*, pp. 2499–2504, 2014.

[17] M.-H. Kang, "A ga-based algorithm for creating an energy-optimum train speed trajectory," *Journal of International Council on Electrical Engineering*, vol. 1, Apr. 2011.

[18] H. Yang, K.-P. Zhang, and H.-E. Liu, "Online regulation of high speed train trajectory control based on t-s fuzzy bilinear model," *IEEE Transactions on Intelligent Transportation Systems*, vol. 17, no. 6, pp. 1496–1508, 2016.

[19] X.-H. Yan, B.-G. Cai, B. Ning, and W. ShangGuan, "Moving horizon optimization of dynamic trajectory planning for high-speed train operation," *IEEE Transactions on Intelligent Transportation Systems*, vol. 17, no. 5, pp. 1258–1270, 2016.

[20] A. Albrecht, P. Howlett, P. Pudney, X. Vu, and P. Zhou, "The key principles of optimal train control—part 2: Existence of an optimal strategy, the local energy minimization principle, uniqueness, computational techniques," *Transportation Research Part B: Methodological*, vol. 94, pp. 509–538, 2016.

[21] P. Howlett, P. Pudney, and X. Vu, "Local energy minimization in optimal train control," *Automatica*, vol. 45, no. 11, pp. 2692–2698, 2009.

[22] S. Lu, M. Wang, P. Weston, C. Shuaixun, and J. Yang, "Partial train speed trajectory optimization using mixed-integer linear programming," *IEEE Transactions on Intelligent Transportation Systems*, vol. 17, pp. 1–10, Mar. 2016.

[23] B. P. Rochard and F. Schmid, "A review of methods to measure and calculate train resistances," *Proceedings of the Institution of Mechanical Engineers, Part F: Journal of Rail and Rapid Transit*, vol. 214, no. 4, pp. 185–199, 2000.

[24] Z. Xiao, Q. Wang, P. Sun, Z. Zhao, Y. Rao, and X. Feng, "Real-time energy-efficient driver advisory system for high-speed trains," *IEEE Transactions on Transportation Electrification*, vol. 7, no. 4, pp. 3163–3172, 2021.

[25] R. Franke, P. Terwiesch, and M. Meyer, "An algorithm for the optimal control of the driving of trains," in *Proceedings of the 39th IEEE Conference on Decision and Control (Cat. No.00CH37187)*, vol. 3, pp. 2123–2128 vol.3, 2000.

[26] M. A. Gozukucuk, T. Akdogan, W. Hussain, T. K. Tasooji, M. Sahin, M. Celik, and H. F. Ugurdag, "Design and simulation of an optimal energy management strategy for plug-in electric vehicles," in *6th International Conference on Control Engineering & Information Technology (CEIT)*, pp. 1–6, 2018.

[27] C. Perkins, "Mazda says its next-generation gasoline engine will run cleaner than an electric car," *Road & Track*, July 2020. [Online]. Available: `https://www.roadandtrack.com/new-cars/car-technology/a15912314/mazda-skyactiv-3-gas-clean-as-ev/`. Accessed: Jun, 2022.

[28] J. Jenkins, "A closer look at the losses in ev motors," *Charged EVs*, Sept. 2021. [Online]. Available: `https://chargedevs.com/features/a-closer-look-at-the-losses-in-ev-motors/`. Accessed: Jul, 2022.

[29] "Bearing friction, power loss and starting torque," *SKF*. [Online]. Available: `https://www.skf.com/au/products/rolling-bearings/principles-of-rolling-bearing-selection/bearing-selection-process/operating-temperature-and-speed/bearing-friction-power-loss-and-starting-torque`. Accessed: Jul, 2022.

[30] "Efficiency and loss mapping of ac motors (whitepaper)," *Charged EVs*. [Online]. Available: `https://chargedevs.com/newswire/the-tech/efficiency-and-loss-mapping-of-ac-motors-whitepaper/`. Accessed: Jun, 2022.

[31] E. Castillo, A. Conejo, P. Pedregal, R. García, and N. Alguacil, "Mixed-integer linear programming," in *Building and Solving Mathematical Programming Models in Engineering and Science*, vol. 3, Jan. 2002.

[32] "Mixed-integer programming (MIP) - a primer on the basics," *Gurobi*. [Online]. Available: `https://www.gurobi.com/resource/mip-basics/`. Accessed: Jan, 2022.

[33] Q. I. Rahman and G. Schmeisser, "Characterization of the speed of convergence of the trapezoidal rule," *Numer. Math.*, vol. 57, p. 123–138, Dec. 1990.

[34] S. ichi Azuma, J. ichi Imura, and T. Sugie, "Lebesgue piecewise affine approximation of nonlinear systems," *Nonlinear Analysis: Hybrid Systems*, vol. 4, no. 1, pp. 92–102, 2010.

[35] A. Bemporad and M. Morari, "Control of systems integrating logic, dynamics, and constraints," *Automatica*, vol. 35, no. 3, pp. 407–427, 1999.

VITA

Name: Burhan Toruk

Languages: Turkish, English

Education

- MS: Ozyegin University, Electrical Electronics Engineering, 2018-Ongoing, CGPA: 3.77/4
- BS: KTO Karatay University, Electrical Electronics Engineering, 2014-2018, CGPA: 3.44/4
- High School: Konya High School (Anatolian)

Work Experience

- FEV Türkiye, Senior Automotive Software Engineer, 2022-Ongoing
- FEV Türkiye, Automotive Software Engineer, 2019-2022
- Özyeğin University, Research Assistant, 2018-2019
- KTO Karatay University, Student Assistant, 2015-2018

Achievements

- Ozyegin University Full Graduate Scholarship, 2018
- TUBITAK Efficiency Challange 2018 Visual Design Award, 2018
- TUBITAK 2209-B Senior Project Contribution for Project BUDA, 2018
- HAVELSAN GIS Solution Competition, 4^{th} Team, Honorable Mention Reward, 2017

- ERASMUS+ Fund, 2016
- KTO Karatay University Electrical-Electronics Engineering, Full Scholarship, 2014